Review of hydrogen–gasoline SI dual fuel engines Engine performance and emission

Article *in* Energy Reports · May 2023

DOI: 10.1016/j.egyr.2023.03.054

5 authors, including:

Sanad Thurakkal Puthan Purayil
United Arab Emirates University
7 PUBLICATIONS **67** CITATIONS
SEE PROFILE

Mohammad O. Hamdan
American University of Sharjah
92 PUBLICATIONS **1,306** CITATIONS
SEE PROFILE

Mohamed Y E Selim
United Arab Emirates University
105 PUBLICATIONS **2,154** CITATIONS
SEE PROFILE

Emad Elnajjar
United Arab Emirates University
73 PUBLICATIONS **1,079** CITATIONS
SEE PROFILE

Energy Reports 9 (2023) 4547–4573

Contents lists available at ScienceDirect

Energy Reports

journal homepage: www.elsevier.com/locate/egyr

Review article

Review of hydrogen–gasoline SI dual fuel engines: Engine performance and emission

S.T.P. Purayil [a], Mohammad O. Hamdan [b], S.A.B. Al-Omari [a], M.Y.E. Selim [a], E. Elnajjar [a,*]

[a] Mechanical Engineering Department, UAE University, Al Ain, United Arab Emirates
[b] American University of Sharjah, University City, Sharjah, United Arab Emirates

ARTICLE INFO

Article history:
Received 18 May 2022
Received in revised form 17 January 2023
Accepted 8 March 2023
Available online xxxx

Keywords:
Hydrogen–gasoline
Dual fuel engine
Combustion
Emission
Cyclic variation
Exhaust gas recirculation

ABSTRACT

Rapid depletion of conventional fossil fuels and increasing environmental concern are demanding an urgent carry out for research to find an alternate fuel which meets the fuel demand with minimum environmental impacts. Hydrogen is considered as one of the important fuel in the near future which meets the above alarming problems. Hydrogen–gasoline dual fuel engines use hydrogen as primary fuel and gasoline as secondary fuel. In this review paper, the combustion performance, emission, and cyclic variation characteristics of a hydrogen–gasoline dual fuel engine have been critically analyzed. According to scientific literature, hydrogen–gasoline dual fuel engines have a good thermal efficiency at low and partial loads, but the performance deteriorates at high loads. Hydrogen direct injection with gasoline port fuel injection is the optimum configuration for dual fuel engine operating on hydrogen and gasoline. This configuration shows superior result in mitigating the abnormal combustion, but experiences high NO_x emission. Employing EGR showed a maximum reduction of 77.8% of NO_x emission with a EGR flowrate of 18%, further increment in flowrate leads to combustion instability. An overview on hydrogen production and carbon footprint related with hydrogen production is also included. This review paper aims to provide comprehensive findings from past works associated with hydrogen–gasoline dual fuel approach in a spark ignition engine.

Contents

* Corresponding author.
E-mail address: Eelnajjar@uaeu.ac.ae (E. Elnajjar).

https://doi.org/10.1016/j.egyr.2023.03.054

1. Introduction

Since the early twentieth century, economies have depended on the transfer of people and goods by internal combustion (IC) engines, which are expected to remain relevant in the coming decades (Shuai et al., 2018; Reitz et al., 2020). Globally, more than 80% of passenger and light-duty vehicles operate using spark ignition (SI) engines, apart from countries like India, the European Union, and South Korea (Yang and Bandivadekar, 2017; Kalghatgi, 2019). The major pollutants from SI engines are CO_2, NO_x and nitrated hydrocarbons (Subramaniam et al., 2020; Zervas et al., 2004). These pollutants cause adverse effects on the environment and human health. Many past studies have reported that cardiovascular and respiratory health problems are caused by excessive concentrations of these pollutants in the human body (D'amato et al., 2016; Kim et al., 2015; Grahame and Schlesinger, 2010). Therefore, emission regulations are becoming more stringent to mitigate these harmful emissions. Furthermore, the rapid depletion of fossil fuels leading to energy crises is also a significant concern (Kim et al., 2014; Yu et al., 2020; Antunes et al., 2008). Scientists and researchers are focused on finding new renewable and environmentally friendly alternative energy sources to mitigate the fast depletion of fossil fuels and environmental concerns (Liu et al., 2021; Kumar and Purayil, 2019; Sun et al., 2019; Zhen and Wang, 2015).

Among the various approaches to overcome the above alarming issues is combining renewable and green fuels with conventional gasoline in an SI engine. The use of hydrogen is a promising way to reduce the dependency on conventional fossil fuels and a favorable approach to addressing emissions issues with several advantages (Ji et al., 2019; Hao et al., 2016; Hamdan et al., 2015). First, hydrogen is available globally at reasonable prices which can be produced easily from renewable sources such as biomass and water splitting (Siddiqui and Dincer, 2021; Pein et al., 2021; Elnajjar et al., 2021b; Lu et al., 2020). Apart from that hydrogen can also be produced through reforming fossil fuel-based products (Holladay et al., 2009). Second, hydrogen is a clean fuel that does not contribute to carbon emissions, such as CO and CO_2 (Subramanian and Thangavel, 2020; Hamdan et al., 2014). Third, hydrogen has a higher research octane number (RON) than conventional gasoline, making it less prone to knocking phenomena. Therefore, hydrogen can be used in dual fuel SI engines and can attain higher thermal efficiencies than engines operating with gasoline alone.

Hydrogen has been employed as both a primary and pilot fuel with conventional gasoline in SI engines because of its environmental and economic benefits (Akal et al., 2020; Navale et al., 2017). Dual fuel injection technology has been widely researched in compression ignition (CI) engines (Sharma and Kaushal, 2021; Lee et al., 2018; Elnajjar et al., 2013, 2021a). However, due to strengthening emission policies worldwide, researchers are forced to introduce new technology or convert the existing technologies to fully operate on clean fuels. As the introduction of new IC engine technology for fully hydrogen use is still an ongoing research due to the low power efficiency compared to the conventional fossil fuel (White et al., 2006). When comparing the emissions from diesel–hydrogen, gasoline–hydrogen emits less exhaust pollutants. In the above aspects of low power efficiency and high emission, hydrogen–gasoline dual fuel technology in SI engine is going to be realistic and profound approach in future (Qian et al., 2022).

This article sets out to review the use of hydrogen–gasoline dual fuel technology in SI engine, while the hydrogen use in CI engine is beyond the scope of this article. Previous works have discussed the use of hydrogen fuel in SI engine along with gasoline, natural gas and alcohols. Akal et al. (2020) reviewed the use of hydrogen and its drawbacks along with the gasoline, LPG and diesel, whereas Gurz et al. (2017) focused on the hydrogen use in IC engine, hybrid-hydrogen IC engine and fuel cell. apart from that, Yan et al. (2018) also reviewed the hydrogen used in SI engine along with the natural gas. On the other hand, there are also few review articles which focused on the recent progress of hydrogen in IC engine and as well as the hydrogen production and its safety measurements when use as a fuel (Sharma and Ghoshal, 2015; Sinigaglia et al., 2017).

A close examination to the above review articles reveals that hydrogen–gasoline use in SI engine is an important subject which is frequently reviewed, in many cases it is not considered as a prime focus and thus the hydrogen–gasoline subject is only briefly explained. Due to the lack of review in the subject and intense ongoing research, it is important to provide a timely comprehensive review.

Following through, this article covers a wide review of detailed findings from recent works based on engine performance, effect of hydrogen–gasoline fraction, effect of EGR and exhaust emissions. Apart from that, the article also provides an overview about the hydrogen production techniques, hydrogen–gasoline induction technology, advantages, and drawbacks of using hydrogen–gasoline fuel in SI engine.

2. Hydrogen as a fuel in internal combustion engines

Hydrogen is a colorless, flammable gas, is the lightest chemical element (Vardar-Schara et al., 2008), and is one of the most abundant elements on Earth, contributing about 0.14% by mass of its crust (Jolly, 2021). Hydrogen production is categorized based on the feedstock used, methods used and greenhouse gas emissions. The conventional for producing hydrogen mainly from methane or natural gas without any greenhouse gas capture is termed grey hydrogen. The hydrogen production through steam methane reforming from natural gas or methane along with the carbon capture and storage is the blue hydrogen. Blue hydrogen is also known as low-carbon hydrogen as it produces less CO_2, whereas CO_2 free hydrogen production through methane pyrolysis is termed turquoise hydrogen. Green hydrogen is one which does not emit any harmful emission during hydrogen production. Green hydrogen is produced from water through electrolysis where the power is derived from clean energy like solar or wind. Whereas when the power for electrolysis is obtained from nuclear energy the production is termed as pink hydrogen. Hydrogen production using lignite and coal through gasification of these resources is termed as brown and black hydrogen (Hermesmann and Müller, 2022; Kakoulaki et al., 2021; Milewski et al., 2021; Sheu et al., 2021). Of the hydrogen production methods, methane reforming currently produces the most hydrogen. The simplest way to produce hydrogen without CO_2 emissions is through the

Nomenclature

AF	Air–Fuel ratio
BMEP	Brake Mean Effective Pressure
BP	Brake Power
BTDC	Before Top Dead Center
BTE	Brake Thermal Efficiency
CA	Crank Angle
CA0-10	Flame development period
CA10-90	Flame propagation period
CCV	Cycle to Cycle Variation
CI	Compression Ignition
CMI	Carburetion Method Induction
CO	Carbon monoxide
CO_2	Carbon dioxide
COV	Coefficient Of Variation
DI	Direct Injection
$dP/d\theta$	Combustion pressure rise rate
dQ	Maximum rate of heat release
EGR	Exhaust Gas Recirculation
GDI	Gasoline Direct Injection
H_2	Hydrogen
HC	Hydrocarbon
HCCI	Homogeneous Charge Compression Ignition
H/C	Hydrogen/Carbon
HHO	Hydroxy gas
HPDI	High-Pressure Direct Injection
HRR	Heat Release Rate
IC	Internal Combustion
IMEP	Indicated Mean Effective Pressure
ITE	Indicated Thermal Efficiency
KOH	Potassium hydroxide
kW	Kilowatt
LHV	Lower Heating Value
L/min	Liter per minute
MAP	Manifold Absolute Pressure
MBT	Minimum spark timing at Best Torque
MEP	Mean Effective Pressure
MPa	Mega Pascal
m/s	Meter per second
N	Engine speed
NaOH	Sodium hydroxide
NO_x	Oxides of Nitrogen
PFI	Port Fuel Injection
PM	Particulate Matter
P_{max}	Maximum pressure
ρ_a	Density of Air
ρ_h	Density of Hydrogen
Q	Heat Transferred
R	Correlation coefficient
RON	Research Octane Number
rpm	Rotations per minute
SFC	Specific Fuel Consumption
SI	Spark Ignition
stoich	Stoichiometric conditions
T	Torque
TiO_2	Titanium dioxide
λ	Excess air ratio
σ_x	Standard deviation of x
K	Kelvin
η	Efficiency
°C	Celsius
$\overline{X}$	Mean Value

Subscript

$\dot{m}_{air}$	Mass flow rate of air
$\dot{m}_{H_2}$	Mass flow rate of hydrogen
$\dot{m}_{gasoline}$	Mass flow rate of gasoline
λ	Excess air ratio
V_G	Flow rate of gasoline
V_{air}	Flow rate of air
V_H	Flow rate of hydrogen
V_{H_2}	Volume of hydrogen
V_{intake}	Intake volume
$\dot{V}_{air}$	Volumetric flow rate of air
$\dot{V}_{H_2}$	Volumetric flow rate of hydrogen
φ_{H_2}	Hydrogen additional fraction
$q_{gasoline}$	Heat produced by gasoline
q_{H_2}	Heat produced by hydrogen
α_{H_2}	Hydrogen energy fraction
Φ	Equivalence ratio

electrolysis of water, which splits water molecules into hydrogen and oxygen using an electric current. Renewable electricity production can achieve complete green hydrogen production in this way.

In hydrogen production from fossil fuels, steam reforming, oxidation of petroleum, reforming of natural gas and gasification of coal (LeValley et al., 2014; Midilli et al., 2021; Silva et al., 2017). Almost 50% of hydrogen production is derived from natural gas, primarily via steam methane reforming. Electrolysis is another form of hydrogen production method falling under the category of water splitting (Chi and Yu, 2018). Electrolysis is an endothermic reaction which requires an input energy provided by electricity. Apart from that, thermolysis is another process for producing hydrogen from water by thermal working at high temperature (Wang et al., 2019). Hydrogen production from biomass is also a promising process, which includes pyrolysis, biomass gasification, bio photolysis and photo fermentation (Yu and Takahashi, 2007; Chang et al., 2011; Uddin et al., 2014).

Apart from that hydrogen is also produced from various byproducts like glycerol and formic acid (Sanni et al., 2021). Glycerol are mainly obtained as a byproduct from biodiesel production and formic acid is an industrial byproduct (Kumar and Purayil, 2019; Wang et al., 2018). Sarma et al. (2012) has conducted a review based on the hydrogen production from glycerol through various microbial process such as microbial fuel cells and bio-electrochemical cells with a maximum hydrogen yield of 6 mol were obtained for one mole of glycerol. From formic acid, established and simplest way for hydrogen production is through decomposition in presence of catalyst (Santos et al., 2021).

Quantifying the carbon footprint has become an important approach in the energy production sector especially in hydrogen production (Akande and Lee, 2022; Sharma et al., 2022). Kim et al. (2021) investigated the estimation on carbon footprint associated with the hydrogen production on each sector starting from the production to inland delivery. Out of those, production and conversion are the sector which account majorly for the

Table 1
Carbon footprint distribution Kim et al. (2021).

Sector	Form	Method	Values/kgCO_2e/kgH_2	
			Minimum	Maximum
Production	Coal	CG with CCS	0.91	5.52
	Natural Gas	SMR with CCS	0.99	9.16
Delivery (50 km)	Coal	Coal railway	0.006	0.01
	Natural Gas	Natural gas pipeline	0.007	0.015
Conversion	Liquid Hydrogen	Regasification	0.46	0.545
		Liquefaction	5.2	6.163
Transportation (5000 km)	Liquid Hydrogen	Liquid Hydrogen Ship	0.50	0.67

total carbon footprint in hydrogen production. Table 1 shows the carbon footprint distribution associated with the hydrogen production mainly from coal, natural gas and liquid hydrogen.

Hydrogen storage is a well-known challenging topic. One of the most common methods for hydrogen storage is accommodating gaseous hydrogen in compressed state in a high-pressure gas cylinder. Another technique is liquefying hydrogen to a lower temperature, but this method is time consuming and less energy efficient. Apart from those few other hydrogen storage techniques include metal hydride, liquid organic hydrogen carriers and metal organic frameworks (Abdalla et al., 2018).

The combustion of hydrogen is clean and does not contribute to added carbon emissions. The first use of hydrogen in IC engines dates to 1806 (Eckermann, 2001). As IC engines using hydrogen fuel are developed, the emission of greenhouse gases from vehicles leading to global warming is expected to decline. Hydrogen possesses a high combustion rate, resulting in less heat lost by heat transfer and increasing thermal efficiency. The detailed properties of hydrogen as a fuel are discussed in the following sections.

2.1. Physicochemical properties of hydrogen and other renewable fuels used in SI engines

The properties of hydrogen and other renewable fuels compatible with the dual fuel mode in SI engines are compared in Table 2 (Yan et al., 2018; Lapuerta et al., 2014; Log and Moi, 2018; Coronado et al., 2012; Zaharin et al., 2018; Bae and Kim, 2017). The renewable fuels compared in Table 2 can be broadly classified as gaseous fuels, liquid fuels, alcohols, furans, and oxygenates. Out of the fuel listed in Table 2, ethanol, methanol, and Iso-butanol fall under liquid, alcohol, and oxygenated category. Whereas hydrogen and methane are gaseous fuels. Gasoline falls under the liquid fuel category. The composition and content of these fuels vary with the source and production process. In addition, the production of some of these fuels can be achieved through fossil fuel processing, such as hydrogen and methane from partial oxidation and steam reforming of natural gas (Muradov, 1993).

RON is a fuel property that characterizes the knock resistance. Higher RON values enable the engine to operate with a higher compression ratio, resulting in improved power output and thermal efficiency. More oxygen content or a lower H/C ratio mitigates the CO and hydrocarbon (HC) emissions. But from the literature, oxygenated fuels with higher latent heats of vaporization and lower heating values (LHVs) could affect the engine performance, resulting in higher brake specific fuel consumption (Pai et al., 2013; Masum et al., 2015). Laminar flame speed is one of the important properties of hydrogen, as it provides an overview of complex combustion process such as flashback, flame stabilization and extinction. In Dong et al. work (Dong et al., 2009), the laminar flame speed of the H_2-air is measured using Bunsen Burner method. This investigation was performed at normal temperature and pressure and calculation was based on reaction zone area and was found out to be 1.85 at an approximate equivalence ratio of 0.9.

From the above fuel comparison, hydrogen is the only carbon-free fuel. Furthermore, hydrogen possesses a high RON, a wide flammability range, and a higher LHV value, allowing hydrogen to run on lean burn characteristics more than any other fuel (Yu et al., 2020). However, some safety issues must be considered when using hydrogen, such as backfire into the intake port due to high laminar flame velocity when hydrogen port injection is employed (Jilakara et al., 2015).

2.2. Hydrogen use in SI engines

Serious effort has been made to enhance the engine combustion system to match evolving emission and fuel economy policies (Santos et al., 2019; Jamrozik and Tutak, 2011). For engines with an ignition source such as SI engines, the fuel must form a homogenous mixture with the incoming air before the electrical discharge ignites the fuel mixture. Based on the introduction of hydrogen into the engine cylinder, the injection systems are mainly classified as:

- Carburetion Method Induction (CMI): In a CMI system, shown in Fig. 1(a) (Al-Baghdadi, 2002), carburetor induction is employed. This is the oldest and simplest technique for hydrogen induction. CMI does not make use of an injector for fuel supply. Here the liquid fuel is discharged through the discharge tube directed towards the carburetor body, where it atomizes in the incoming air. Hydrogen is introduced before the throttle valve and is mixed with the air–fuel mixture before entering the intake manifold.
- Port Fuel Injection (PFI): In a PFI system, shown in Fig. 1(b) (Kalwar and Agarwal, 2020), a required quantity of fuel is sprayed by the nozzle into the intake manifold, which is carried away by the incoming air to the engine cylinder (Steinbrecher et al., 2016). In a PFI system, the fuel is introduced in two ways: single-point and multi-point injection. The fuel is injected to a common point in the intake manifold serving all the cylinders in single-point injection. By contrast, in multi-point injection, an even quantity of fuel is injected near the intake valve of each cylinder. In a PFI system, the hydrogen is injected into the intake manifold directed towards inlet valve and liquid fuel is introduced either to the same manifold or through direct injection to the combustion chamber.
- Direct Injection (DI): In a DI system, shown in Fig. 1(c) (Kalwar and Agarwal, 2020), fuel is injected directly into the combustion chamber with a high-pressure injector, sometimes known as high-pressure direct injection (HPDI). DI systems are typically employed based on two combustion modes: stratified lean combustion mode and homogenous stoichiometric combustion mode (Lee et al., 2020). The stoichiometric combustion mode injects fuel before the electrical discharge to form a homogenous mixture, and injection

Table 2
Physicochemical properties of hydrogen and other renewable fuels Yan et al. (2018),Lapuerta et al. (2014), Log and Moi (2018), Coronado et al. (2012), Zaharin et al. (2018), Bae and Kim (2017).

Properties	Hydrogen	Gasoline	Ethanol	Methanol	Iso-butanol	Methane
Chemical formula	H_2	$C_4 - C_{12}$	C_2H_5OH	CH_3OH	C_4H_9OH	CH_4
Molar mass (g/mol)	2	60–170	46	32	74	2.5
H/C ratio	0	1.7–1.9	3	4	2.5	4
Oxygen content (wt%)	0	0	34.7	50	21.6	0
Density (g/cm^3)	0.0013@ 15 °C	0.748 @ 15 °C	0.794 @ 15 °C	0.796 @ 20 °C	0.811 @ 15 °C	0.72 @ 20 °C
Dynamic viscosity (mPa s)	0.009	0.37–0.44	1.5	0.6	8.3	0.01
Boiling point (°C)	−253	25–210	78	65	108	−162
Auto-ignition temperature (°C)	572	256	363	385	415	540
LHV (MJ/kg)	120	44.1	28.8	19.7	35.54	50
Latent heat of vaporization (kJ/kg)	448	349	923	1110	683	510
RON	130	95	107.4	109	105.1	120
Laminar flame speed (m/s)	1.85	0.37–0.43	0.39	0.56	0.45	0.38
Flammability limits in air (vol%) (lower-higher)	4.0–75	1.2–6.0	3.3–19	6.7–36	1.7–12.0	5.3–15
Minimum ignition energy (mJ)	0.02	0.25	0.28	0.14	–	0.28
Diffusion coefficient (cm^2/s)	0.61	–	0.135	0.152	0.0865	0.189

normally occurs during the intake stroke. Fuel is injected into two regions in the stratified lean combustion mode: a rich mixture near the spark plugs and a lean mixture in other regions. In a DI system, the hydrogen is injected directly into the combustion chamber, and the liquid fuel is introduced either into the intake manifold or directly into the combustion chamber with a secondary injector.

As stated earlier, fuel is injected directly into the combustion chamber in DI injection, which reduces the time lag and enhances the transient response. The fuel evaporation within the cylinder cools the surroundings, enhancing the volumetric efficiency and reducing the knock intensity. The DI injection mode can operate at higher compression ratios, enhancing thermal efficiency (Chen et al., 2011). Many studies have reported that the DI injection mode can increase thermal efficiency (Melaika et al., 2021; Kim et al., 2020; Zhang et al., 2018). Table 3 shows the hydrogen and gasoline dual fuel induction techniques employed in SI engines reported in past works.

When comparing the induction system to introduce hydrogen, both DI and PFI injection have their own advantages. But the best configuration for hydrogen–gasoline dual fuel method, hydrogen DI and gasoline PFI is desired. In this configuration, high in-cylinder pressure, higher brake thermal efficiency and reduced brake specific fuel consumption can be obtained. This was mainly due to increased turbulence in the cylinder and high volumetric efficiency. The heat release rate depends on the latent heat, calorific value, and combustion temperature. Due to the increased combustion temperature in the above configuration, high heat release rate is observed. In terms of emission like HC and NO_x, hydrogen DI is not that efficient compared to hydrogen PFI. This is mainly due to high in-cylinder temperature. Apart from that the reduction in engine performance in hydrogen PFI and gasoline DI was mainly due to high air displacement which resulted in lower volumetric efficiency (Aghahasani et al., 2022; Catapano et al., 2016).

2.3. Hydrogen supply fraction terminology

Hydrogen fraction is one of the important parameters influencing performance and emission characteristics. As per past work on hydrogen–gasoline dual fuel method, the hydrogen fraction varied as 3% (Ji et al., 2012), 5% (Du et al., 2017), 8% (Ji and Wang, 2011), 9% (Shi et al., 2017), 12% (Sun et al., 2016), 20% (Yu et al., 2019b) and 31% (Elsemary et al., 2017). Apart from that an excess air ratio 1.2 is also considered as optimum condition (Niu et al., 2016; Liang, 2019; Yu et al., 2019a). Ganesan et al. (2022) conduced an optimization study on SI engine operating with gasohol (80% gasoline and 20% methanol)-hydrogen blend using Response Surface Methodology (RSM). This research work was aimed at identifying the optimum hydrogen fraction and engine speed based on BSFC, BTE, CO, HC and CO_2. Hydrogen fraction of 20% at an engine speed of 1500rpm superior results were obtained, which was confirmed using a validation test. This section describes the fraction of hydrogen/gasoline supplied to a SI engine based on the dual fuel mode.

2.3.1. Excess air ratio (λ) (Niu et al., 2016)

$$\lambda = \frac{\dot{m}_{air}}{\dot{m}_{H_2} AF_{H_2} + \dot{m}_{gasoline} AF_{gasoline}} \quad (1)$$

where $\dot{m}_{air}$, $\dot{m}_{H_2}$, and $\dot{m}_{gasoline}$ represent the mass flow rates of air, hydrogen, and gasoline, respectively. AF_{H_2} and $AF_{gasoline}$ represent the stoichiometric air–fuel ratios of hydrogen and gasoline respectively, where $AF_{H_2} = 34.3$ and $AF_{gasoline} = 14.7$.

2.3.2. Hydrogen additional fraction (φ_{H_2}) (Niu et al., 2016)

$$\varphi_{H_2} = \frac{\dot{V}_{H_2}}{\dot{V}_{H_2} + \dot{V}_{air}} \quad (2)$$

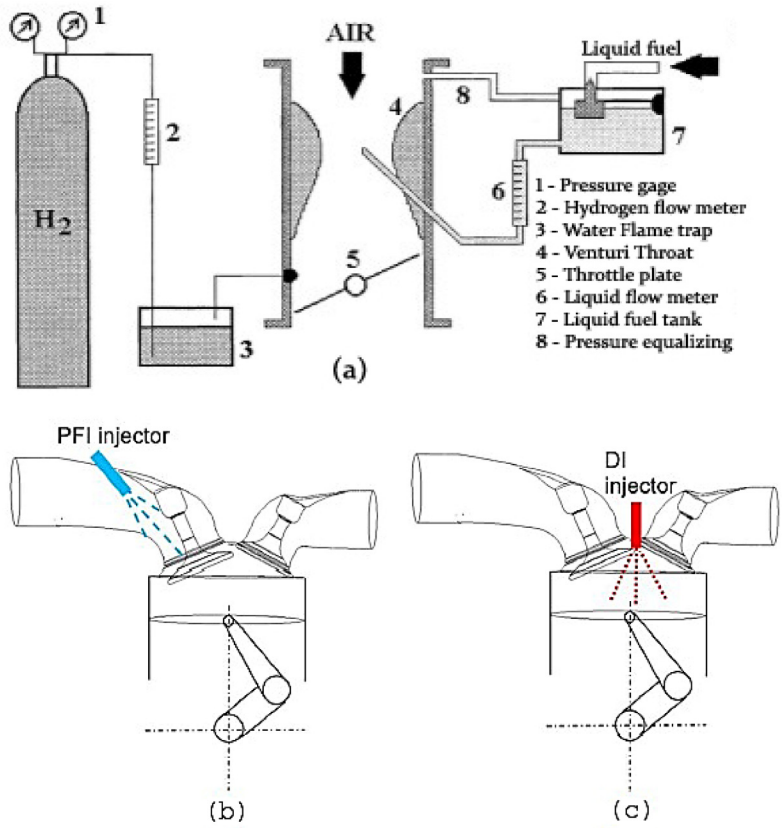

Fig. 1. Engine fuel injection configurations (Al-Baghdadi, 2002; Huang et al., 2021): (a) carburetion method induction (CMI); (b) port fuel injection (PFI); (c) direct injection (DI).

where $\dot{V}_{H_2}$ and $\dot{V}_{air}$ represent the volumetric flow rates of hydrogen and air, respectively. The hydrogen additional fraction can also be represented as

$$\varphi_{H_2} = \frac{\dot{m}_{H_2}}{\dot{m}_{H_2} + \dot{m}_{air}\frac{\rho_h}{\rho_a}} \tag{3}$$

where $\dot{m}_{air}$ and $\dot{m}_{H_2}$ represent the mass flow rates of air and hydrogen, respectively, and $\frac{\rho_h}{\rho_a}$ represents the density ratio of hydrogen to air which has a constant value of $\frac{2}{29}$.

2.3.3. Equivalence ratio (Φ) (D'andrea et al., 2004)

$$\Phi = \frac{\dot{V}_G / \left[\dot{V}_{Air} - \frac{\dot{V}_H}{(C_H/C_{Air})_{stoich}}\right]}{(C_G/C_{Air})_{stoich}} \tag{4}$$

where $\dot{V}_G$, $\dot{V}_{Air}$ and $\dot{V}_H$ represent the flow rates of gasoline, air, and hydrogen, respectively. C_G, C_H and C_{Air} represent the concentrations of gasoline, hydrogen, and air, respectively. The subscript stoich denotes stoichiometric conditions. The molar mean value of $(C_G/C_{Air})_{st}$ is to be 0.42. The term $\dot{V}_H/(C_H/C_{Air})_{st}$ indicate the amount of air required for complete hydrogen oxidation.

2.3.4. Hydrogen energy fraction (α_{H_2}) (Yu et al., 2019a)

$$\alpha_{H_2} = \frac{q_{H_2}}{q_{H_2} + q_{gasoline}} = \frac{\dot{m}_{H_2} * LHV_{H_2}}{\left(\dot{m}_{H_2} * LHV_{H_2}\right) + \left(\dot{m}_{gasoline} * LHV_{gasoline}\right)} \tag{5}$$

where q_{H_2} and $q_{gasoline}$ represent the heat produced by the hydrogen and gasoline, respectively.

2.3.5. Volume rate of hydrogen (α_{H_2}) (Zhang et al., 2020)

$$\alpha_{H_2} = \frac{V_{H_2}}{V_{intake}} \tag{6}$$

where V_{H_2} and V_{intake} represent the intake hydrogen volume for each cycle and the intake volume at the end of the intake process.

The stochiometric ratio is the precise ratio of air to fuel at which complete combustion occurs. Whereas the ratio of actual air to fuel ratio is the excess air ratio. Apart from that, another terminology used is the equivalence ratio, which is the reciprocal of excess air ratio. The stochiometric ratio of hydrogen is 34.3:1 by mass (Niu et al., 2016). This indicates that for one kilogram of hydrogen 34.3 kilogram of air is required, which is higher than for gasoline (14.7:1). So, any value beyond 34.3 is considered as the lean combustion and any value less than 34.3 is rich combustion. But due hydrogen's wide flammability range, hydrogen fueled engine can operate anywhere between the ratios of 34.3:1 and 180:1, but to run on ultra-lean mixture it requires special consideration (Kumar et al., 2015). For stoichiometric combustion, the space occupied by the hydrogen in combustion chamber is calculated as:

$$\text{Hydrogen}\,(\%) = \frac{V_{H2}}{V_{Total}} x100 = \frac{\text{mole of } H_2}{\text{mole of } H_2 + \text{moles of air}}\ x100 = 29.6\%$$

So, based on the engine capacity and load, the hydrogen fraction at which it occupies 29.6% of combustion chamber can be considered as the optimum upper hydrogen fraction limit.

Table 3
Hydrogen and gasoline dual fuel induction techniques in past work.

Sl. no	Authors	Engine specifications		Hydrogen induction system	Gasoline Induction system	Main findings
		Displacement	Air intake system			
1	Wang et al, 2011. Wang et al. (2011)	1.6 L, 4 stroke	Aspirated	PFI	DI	• Cold start properties increased. • NO_x increased.
2	Nguyen, 2013. Nguyen (2013)	97 cc, 4 stroke	Aspirated	PFI	Carburetor	• Engine power increased. • HC reduced. • NO_x and CO increased
3	Shivaprasad et al, 2014. Shivaprasad et al. (2014)	338 cc, 4 stroke	Aspirated	PFI	PFI	• BTE and BMEP increased. • HC and CO reduced. • NO_x increased.
4	El-Kassaby et al, 2016. El-Kassaby et al. (2016)	1.3 L, 4 stroke	Aspirated	PFI	DI	• Thermal efficiency increased. • NO_x, CO and HC reduced.
5	Sun et al, 2016. Sun et al. (2016)	1.8 L, 4 stroke	Aspirated	DI	PFI	• In-cylinder pressure increased. • Total particle number reduced.
6	Elsemary et al, 2016. Elsemary et al. (2016)	389 cc, 4 stroke	Aspirated	PFI	Carburetor	• BTE increased. • HC and CO increased.
7	Niu et al, 2016. Niu et al. (2016)	1.8 L, 4 stroke	Aspirated	DI	PFI	• In-cylinder pressure and HRR increased. • Effective thermal efficiency increased. • HC and CO reduced. • NO_x increased.
8	Yu et al, 2016. Yu et al. (2016)	1.8 L, 4 stroke	Aspirated	DI	PFI	• Hydrogen DI benefits stratified mixture. • COV reduced.
9	Ji et al, 2018. Ji et al. (2018)	1.6 L, 4 stroke	Aspirated	PFI	DI	• BMEP reduced. • CA0-10 and CA10-90 shortened. • NO_x increased.
10	Kim et al, 2018. Kim et al. (2018)	2.0 L, 4 stroke	Turbocharged	PFI	DI	• Cycle to cycle variation improved. • Indicated thermal efficiency increased.
11	Liang, 2019 Liang (2019)	1.8 L, 4 stroke	Aspirated	DI	PFI	• Peak cylinder pressure timing retarded. • Cylinder temperature increased.
12	Bas et al, 2020. BAŞ et al. (2020)	661 cc, 4 stroke	Aspirated	Carburetor	Carburetor	• Unburned HC reduced. • CO_2 andNO_x increased

2.4. Hydrogen fuel: Challenges and drawback

Hydrogen as a fuel is superior in terms of performance and part of emission for an IC engine. However, its use has a high probability of backfire, which deteriorates the power increase. Apart from that, backfire causes mild to severe damage to the engine, and it leads to other abnormal combustion like knock and preignition (Yang et al., 2022). The factors responsible for backfire initially cause preignition which then turns to backfire.

Recent research works have reported on the control methods of backfire associated with hydrogen use (Dhyani and Subramanian, 2021, 2018, 2019). However, most of the control methods result in power degradation, low combustion temperature and low volumetric efficiency. Many control methods such as adjusting fuel timing, spark timing, operating on lean conditions and EGR have both good and bad side for backfire control. These method lowers the combustion temperature reducing the chance for hotspots, but methods may widen the intake process if improperly judged. Apart from that, isolating the individual intake manifold and connecting to corresponding intake ports has shown better control over backfire without any aftereffects, but this approach for an existing engine results in extra expenditure (Gao et al., 2022). To further reduce the aftereffect of backfire control, multiple methods for backfire control are recommended.

2.5. Hydrogen mixture formation

Mixture Formation for a hydrogen fueled engine is of much importance especially due to its low ignition energy, rapid burning characteristics and short quenching distance, which are prime factors for backfire and preignition. Apart from that, any hotspot like tip of spark plug, hot valves and valve seats works as a source for abnormal combustion (Stępień, 2021). In a SI engine, the air–fuel mixing strategy is classified based on the location for fuel dosing. It is classified as external mixture formation (mixing outside the combustion chamber) or internal mixture formation (mixing inside the combustion chamber) (Rana et al., 2015).

External mixture formation is normally employed using venturi carburation, sequential injection, and throttle body injection (Pandey and Kumar, 2022; Ma and Wang, 2008; Bhola, 2011). For hydrogen fueled engines, throttle body injection and venturi carburation are not much recommended, as there is always a chance for hotspot which may lead to backfire. Hydrogen injection to intake manifold is another less risk strategy. This strategy can achieve better mixing with less prone to abnormal combustion.

In internal mixture formation, hydrogen direct injection is the best strategy. In DI, the hydrogen is injected directly inside the combustion chamber with needed pressure towards the end

Table 4
PFI+DI and PFI+PFI dual fuel induction techniques in past work.

Sl no.	Authors	Engine specifications		Dual fuel induction system	Main findings
		Displacement	Air intake system		
1	Namho et al, 2014. Kim et al. (2014)	500cc, 4 stroke	Aspirated	PFI-Ethanol DI-Gasoline	• Lower knock at high ethanol injection. • NO_x increased as ethanol increased.
2	Feng et al, 2018. Feng et al. (2018)	500cc, 4 stroke	Aspirated	PFI-Gasoline DI-n-butanol	• 2.2% higher engine IMEP. • n-butanol DI led to maximum combustion pressure.
3	Eshan Singh et al, 2019. Singh et al. (2019)	454cc, 4 stroke	Turbocharged	PFI-Methane DI-Gasoline	• At optimum spark, 5% increase in Indicated specific fuel consumption. • NO_x was constant with increasing load.
4	Changming et al, 2020. Gong et al. (2020)	1.798L, 4 stroke	Aspirated	PFI-Hydrogen DI-Methanol	• Hydrogen reduced combustion duration. • Brake Specific Hydrocarbon decreased as excess air ratio increased.
5	Roberto et al, 2019. da Costa et al. (2019)	454cc, 4 stroke	Aspirated	PFI-CNG PFI-Ethanol	• Better fuel conversion efficiency. • NO_x emission increased.
6	Changming et al, 2019. Gong et al. (2019)	125cc, 4 stroke	Aspirated	PFI-LPG PFI-Methanol	• At low temperature, LPG determines the reliable firing.

of compression stroke. This is the most efficient strategy out of all for the hydrogen supply. The DI is further classified as wall-guided, jet-guided and air guided concepts (Rana et al., 2015).

3. Dual fuel injection engines

As stated earlier, dual fuel injection technology has been studied widely for CI engines. In dual fuel technology there are mainly three types of configurations, DI+DI, PFI+PFI and DI+PFI. Out of these configurations, DI+PFI and PFI+PFI have been extensively explored. Due to the larger size of hydrogen injector and limited space for injection area, the DI+DI configuration are not much used (Sáinz et al., 2012). Feng et al. (2018) studied combustion performance on n-butanol DI and gasoline PFI in an SI engine, noting a decrease in knock occurrence with increasing n-butanol mass fraction but at the cost of a higher fuel consumption rate. Dong et al. (2009) investigated knock, and EGR limit extension on a boosted SI engine with gasoline DI and ethanol PFI for a boosted atmospheric condition. *The authors were able to achieve short duration and enhanced combustion stability using dual fuel injection, but an increase knock intensity was observed due to increased unburned gas temperature.* Kang et al. (2019) investigated knock suppression and combustion performance for a dual fuel, dual injection engine using gasoline and ethanol. The dual injection mode resulted in wide engine load characteristics compared to PFI+DI and gasoline direct injection (GDI) modes, but dual injection resulted in high knock tendency, mainly due to higher brake mean effective pressure (BMEP). The combustion improved with further increases in ethanol mass fraction, resulting in higher thermal efficiency.

The dual fuel concept is superior to GDI in many ways, which includes enhanced cooling effects, knock reduction, engine flexibility, extended lean burn conditions, and increased thermal efficiency. The cooling effect and knock mitigation mainly depend on the fuel used, with higher RON reducing the knock intensity. In addition, DI injection in dual fuel systems also contributes to knock reduction. Dual fuel DI has a robust cooling effect compared to PFI because of the fuel evaporation within the combustion chamber. Such cooling effects result in enhanced volumetric and thermal efficiency, reduced NO_x emissions, and knock mitigation. Higher compression ratios than conventional gasoline-fueled engines can also be achieved (Nwovu et al., 2018; Kasseris and Heywood, 2012).

Compared with GDI, dual fuel engines can switch their fuel supply between PFI and DI to achieve optimal output under various operating conditions. DI alone can be used for cold starting to ensure the oversupply of fuel with PFI to reduce fuel consumption and HC emissions. While employing PFI, wetting of intake port wall may cause a time lag between the fuel injection and fuel delivery. This leads to slow transient response and metering errors, especially over fueling is favorable during cold start which results in poor efficiency and increased HC emissions. The engine can mainly use PFI at low load operating conditions to avoid poor evaporation of directly injected fuel due to low in-cylinder temperatures. By contrast, the dual fuel mode can switch to DI as the primary injection source to suppress knock intensity with enhanced cooling effects at increased load conditions. Lean burn is an effective strategy to optimize the fuel economy and reduce NO_x emissions. The extension of the lean burn limit depends mainly on the fuel being injected. Hydrogen utilization offers the ability to adjust to the limits of lean burn combustion more than any other fuel. This is mainly because of the rapid flame velocity, low ignition energy, wide flammability limit, and faster diffusion rate of hydrogen (Yilmaz, 2021; Su et al., 2018, 2017b) (see Table 4).

4. Combustion, performance, and emission characteristics of a hydrogen/gasoline dual fuel engine

A hydrogen–gasoline dual fuel engine's combustion, performance, and emissions characteristics are determined mainly by its design parameters and operating conditions. The influences of parameters such as engine speed, engine load, spark timing, hydrogen–gasoline composition ratio, excess air ratio, EGR flow rate, and cyclic variation on the combustion, performance, and emission characteristics have been investigated.

4.1. Effect of engine speed

Engine speed is one of the key parameters affecting engine combustion behavior (Hagos et al., 2014). Air–fuel mixing, combustion duration, upshifting and downshifting of gears, and cold start characteristics are all influenced by the engine speed. In addition, the signals from the engine speed sensors are needed to investigate engine vibration and noise tracking (Baillie, 2010). Adding hydrogen to an SI engine helps attain better combustion stability and improved cold start characteristics. In hydrogen–gasoline dual fuel engines, improvements in the indicated thermal efficiency were more pronounced at the idle speed than in normal driving conditions (Wang et al., 2011). By contrast, increasing engine speeds increases the emission characteristics as large fuel concentrations are supplied.

Table 5
Detailed experimental conditions for various hydrogen–gasoline tests Ji et al. (2012).

Test number	Working conditions	Type of fuels	λ	α_{H_2} (%)
C1	Cold start	Pure gasoline	–	–
C2	Cold start	Pure hydrogen	–	–
I1	Idle	Pure gasoline	1.00	0.00
I2	Idle	Hydrogen + gasoline	1.00	3.23
I3	Idle	Pure gasoline	1.36	0.00
I4	Idle	Hydrogen + gasoline	1.37	3.00
N1	1400 rpm, MAP = 36.8 kPa	Pure gasoline	1.20	0.00
N2	1400 rpm, MAP = 36.8 kPa	Hydrogen + gasoline	1.20	3.00
N3	1400 rpm, MAP = 86.5 kPa	Pure gasoline	1.20	0.00
N4	1400 rpm, MAP = 86.5 kPa	Hydrogen + gasoline	1.20	3.00

Wang et al. (2011) investigated the starting characteristics of SI engines fueled with a gasoline–hydrogen mixture. The experimental runs were conducted with pure gasoline and 2.5 and 4.5 Liter per minute (L/min) hydrogen addition. The results showed that the engine speed increased from 2017 rpm for pure gasoline to 2048 and 2144 rpm with 2.5 and 4.3 L/min hydrogen, respectively. However, the high diffusion and rapid combustion characteristics of hydrogen also helped to reduce the combustion duration. The number of cycles required to attain peak engine speed was reduced with hydrogen addition to the eighth cycle for 2.5 L/min of hydrogen and the sixth cycle for 4.3 L/min of hydrogen, whereas the peak engine speed for the gasoline-only operation was obtained at the tenth cycle. All test fuels showed similar behavior after 20 cycles.

Ji et al. (2012) examined the addition of hydrogen in a hybrid engine at two different speed conditions: idle speed (790 rpm) and city speed (1400 rpm). The different cases are shown in Table 5. The indicated thermal efficiency (ITE) was improved with hydrogen addition, as shown in Fig. 2. This effect occurred primarily because hydrogen was burned more completely than gasoline because of its short quenching distance and wide flammability. With increased speed, chemical and physical delays are reduced because of turbulence enhancement (Ashok et al., 2015; Alam et al., 2001).

Kamil and Rahman (2015) compared the engine performance of hydrogen–gasoline and hydrogen–methane fueled SI engines with 5%, 10%, 15%, and 20% hydrogen mass fractions at stoichiometric conditions. The results showed decreased brake power (BP) with increasing hydrogen fraction. At 3000 rpm, a BP reduction of 0.56 W was observed, with a 1.33 W reduction at 7000 rpm. This deterioration was due to the lower energy density of the mixture when hydrogen was added. However, a drop in maximum cylinder temperature and power output was observed beyond 5000 rpm for the same hydrogen mass fraction. This drop occurred because the intake charge velocity reached the sonic condition known as choked flow. Choked flow is mainly observed in restricted paths, typically near the intake valve (Kahraman et al., 2009; Ceper et al., 2009).

BMEP is an engine parameter that influences the engine power output (Shivaprasad et al., 2014; Winterbone and Turan, 2015). Shivaprasad et al. (2014) investigated the effect of hydrogen addition on BMEP characteristics as a function of engine speed. The authors varied the hydrogen mass fraction from 0% to 25% at 5% increments. The results showed that BMEP rises as the hydrogen fraction increases, as shown in Fig. 3(a). This trend was due to a wide flammable range and higher adiabatic flame temperature, which helps to achieve rapid and complete combustion. The authors also studied the effect of emission characteristics at different engine speeds. They observed minimum NO_x for 5% hydrogen fraction, but NO_x showed higher emissions than pure gasoline for all hydrogen fractions, as depicted in Fig. 3(b). The main reason for this increase in NO_x emissions is the increased cylinder temperature. The results for CO (Fig. 3(c)) showed a

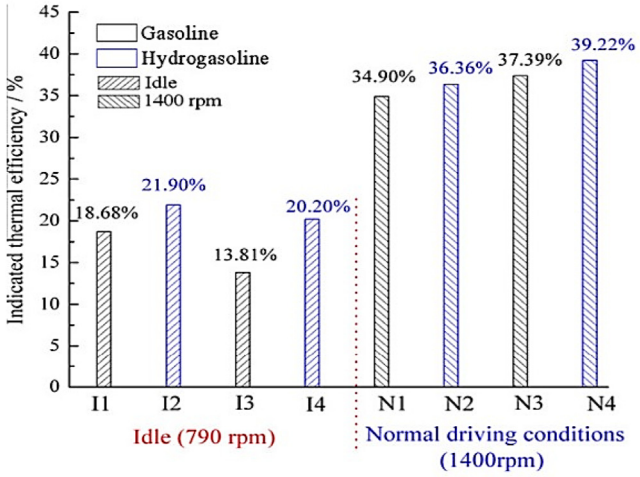

Fig. 2. Histogram of indicated thermal efficiency (ITE) for different hydrogen–gasoline tests (Ji et al., 2012).

reduction with increasing hydrogen fraction. The minimum CO emission (<1%) was observed for a 25% hydrogen fraction because the hydrogen enrichment helped to enhance combustion. From Fig. 3(d), it is evident that HC emissions follow a similar trend to CO, with increased hydrogen fraction corresponding to a reduction in HC emissions. This was mainly due to the short quenching distance that allowed the flame to travel near the cylinder wall, promoting complete combustion.

In addition, researchers have also tried to incorporate onboard hydrogen or hydrogen-rich gas production for SI engine applications. Hydroxy (HHO) gas is normally consisting of unseparated oxygen and hydrogen (monoatomic state) which are obtained by the water electrolysis using catalysts like NaOH and KOH. After ignition, the high combustion temperature splits the hydrogen and oxygen atoms out of HHO gas. Due to the presence of this oxygen, the auto-ignition temperature of HHO gas is less than that of pure hydrogen. This low auto-ignition temperature and low ignition energy of HHO gas, which are the reducing function of equivalence ratio, resulting in the increased risk for knock and preignition (Yilmaz et al., 2010). But with HHO gas, the octane rating of gasoline fuel can be improved. This helps in increasing the compression ratio for obtaining higher efficiency. El-Kassaby et al. (2016) experimentally investigated the optimization of HHO onboard gas production from water as a fuel for an SI engine application. The HHO gas production was accomplished using sodium hydroxide (NaOH) and potassium hydroxide (KOH) catalysts. The optimum catalyst levels were 4 g/L for NaOH and 6 g/L for KOH. Fig. 4 shows the variation in the average efficiency of the HHO gas cell versus engine speed at the optimized catalyst levels. The results showed that the average efficiency was higher for the KOH catalyst than for the NaOH catalyst at different engine

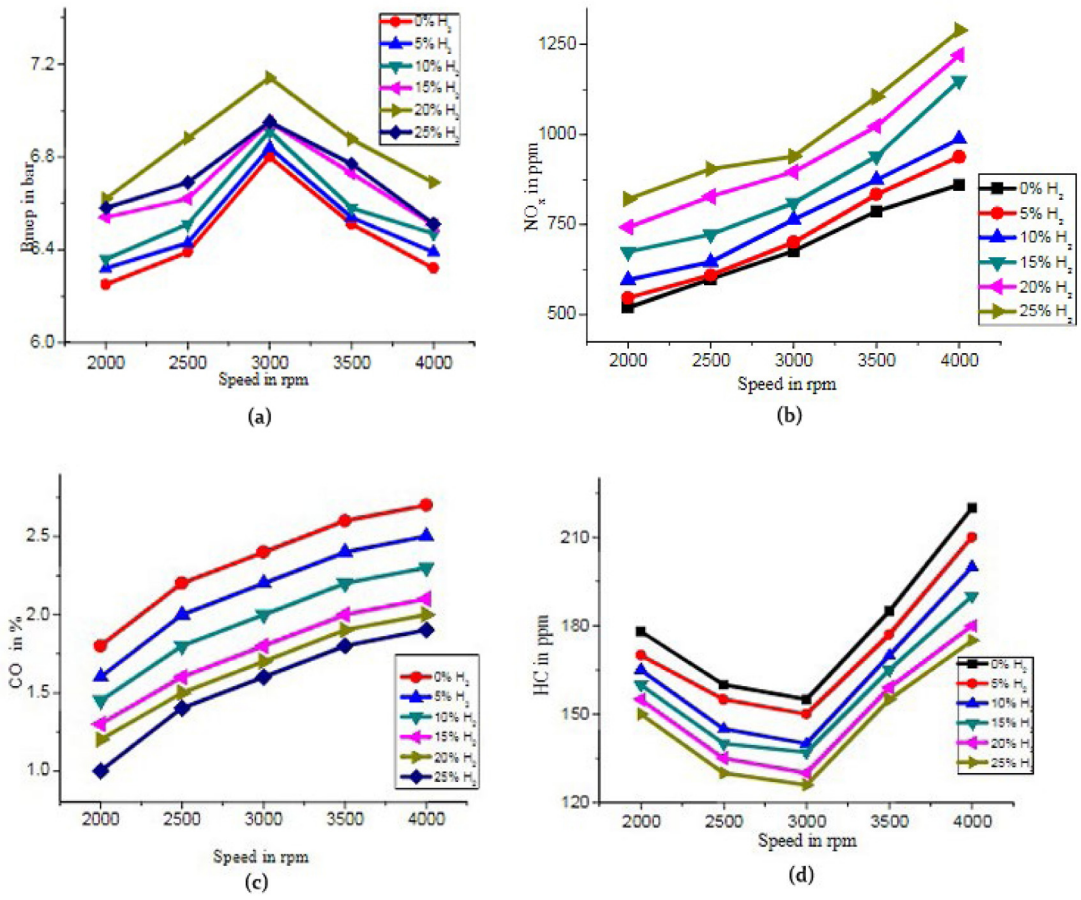

Fig. 3. Variation of (a) BMEP, (b) NO_x (c) CO and (d) HC emissions with engine speed at different hydrogen fractions (Shivaprasad et al., 2014).

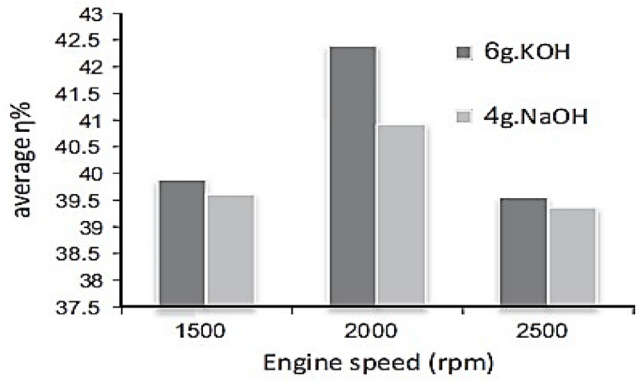

Fig. 4. Variation of average efficiency of onboard HHO gas cell versus engine speed at two optimized catalyst levels (El-Kassaby et al., 2016).

speeds. This high efficiency can be attributed to the use of high concentration of KOH. As the concentration of catalyst increases the ionic conductivity of the used water increases which could result in high HHO availability for combustion (Essuman et al., 2019) (see Table 6).

4.2. Effect of engine torque/engine load

Good torque characteristics are obtained at low excess air ratios in hydrogen–gasoline dual fuel engines because rich burn conditions provide more fuel for combustion to cope with high engine demand (Ji and Wang, 2011). The addition of hydrogen enhances the torque, and ignition timing advances to attain peak torque (Du et al., 2017). Hydrogen addition has been used to enhance the performance of lean burn conditions operating at low speed and low load to improve the fuel consumption of SI engines (Ji and Wang, 2011; Nguyen et al., 2021).

Ji and Wang (2011) investigated the effect of hydrogen enrichment on an SI gasoline engine at low loads and lean burn characteristics. The engine was operated at a constant speed of 800 rpm for three hydrogen volume fractions (3%, 5%, and 8%) and four excess air ratios (1.00, 1.18, 1.43, and 1.67). The results showed a significant increase in brake thermal efficiency (BTE) and torque, as shown in Fig. 5. For a given excess air ratio, torque increased with increasing hydrogen volume fraction because rapid combustion and high diffusion characteristics promoted the degree of constant volume combustion and high combustion velocity reduced the exhaust losses due to the reduced post-combustion period. In addition, these characteristics of hydrogen also helped in a noticeable reduction in cyclic variation, which is more pronounced at low load and lean burn conditions.

The enhancement of engine performance at a low speed and partial load is more pronounced than at a high speed and high load, meaning that hydrogen enrichment during the intake process is more beneficial for engines operating at partial load (Du et al., 2017; Wang et al., 2010). For partial load operating conditions, Su et al. (2017c) studied the effect of hydrogen–gasoline rotary engine performance under lean conditions. A manifold absolute pressure (MAP) of 35 kPa, engine speed of 4500 rpm, and spark advancement of 25° CA were adopted. From Fig. 6(a)–(b), it is evident that hydrogen addition resulted in significant

Table 6
Summary of the effects of engine speed.

References	Engine specification	Hydrogen induction system	Hydrogen fraction	Result
Wang et al, 2011. Wang et al. (2011)	1.6 L, 4 stroke	PFI	2.5 and 4.3 L/min	• Enhancement of engine speed with hydrogen addition. • Reduction in number of cycles to attain peak engine speed.
Shivaprasad et al, 2014. Shivaprasad et al. (2014)	338 cc, 4 stroke	PFI	5% to 25% (5% intervals)	• BMEP and NO_x emission increased as hydrogen fraction increased. • CO and HC emissions decreased as hydrogen fraction increased.
El-Kassaby et al, 2016. El-Kassaby et al. (2016)	1.3 L, 4 stroke	PFI	HHO gas	• HHO cells can be easily incorporated into existing engines. • Best optimized value of catalyst was found to be 6g/L KOH.
Ji et al, 2012. Ji et al. (2012)	1.6 L, 4 stroke	PFI	3% and 3.2%	• Increase in ITE. • Hydrogen addition was much more pronounced at idle conditions.
Kamil et al, 2015. Kamil and Rahman (2015)	149.8 cc, 4 stroke	PFI	5% to 20% (5% intervals)	• Decrease in BP as hydrogen fraction increased. • Reduction in power output beyond 5000 rpm.

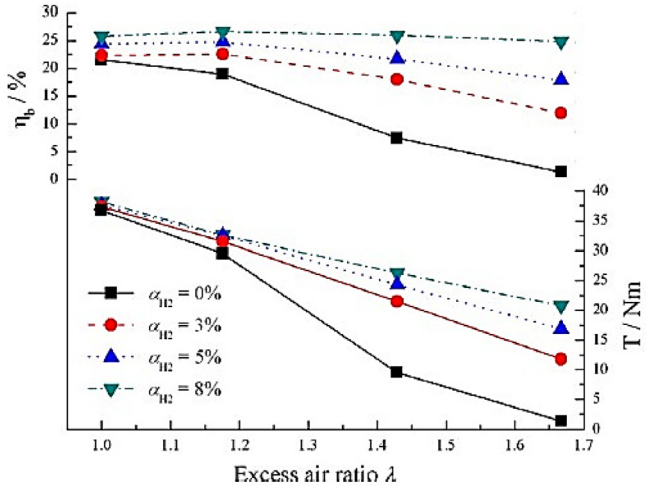

Fig. 5. Brake thermal efficiency (BTE) and torque versus excess air ratio at 800 rpm for three hydrogen enrichment levels (Ji and Wang, 2011).

improvement for BMEP and thermal efficiency for all excess air ratios compared with pure gasoline. This is because the wide flammability range of hydrogen helped in the combustion of the hydrogen–gasoline mixture, resulting in more complete combustion. However, for further increases in excess air ratio, BMEP and thermal efficiency decreases. The excess air ratio beyond 1.2 a major reduction in thermal efficiency and BMEP was observed from Figs. 5 and 6, same excess fuel ratio of 1.2 was considered as optimum in upcoming Section 4.5. This is because of the low volumetric energy density of hydrogen which results in a lower energy mixture in the combustion chamber.

Du et al. (2017) investigated the effect of EGR on power performance for a single-cylinder engine with gasoline PFI and hydrogen DI. Fig. 7(a) and (b) show the variations of torque and ignition timing for hydrogen enrichment. Hydrogen addition resulted in a significant torque increase for a given ignition timing and EGR flow rate. For 15 °CA BTDC and a 0% EGR ratio, the torque generated by pure gasoline combustion is 77.4 N-m, compared to 87.7 N-m with 5% hydrogen addition. A further increase beyond 5% hydrogen addition resulted in no apparent change in torque. Similarly, the torque began decreasing after an ignition timing of 16° CA BTDC.

In an SI engine, two conditions are observed for hydrogen in the engine cylinder: homogenous and stratified conditions. Yu et al. (2019b) investigated the effect of stratified and homogenous hydrogen conditions on combustion in a gasoline–hydrogen fueled SI engine. As reported in the above literature, the same trend of increased torque with hydrogen addition was observed, with stratified conditions slightly better than homogenous conditions. This is because the hydrogen concentration in the vicinity of the spark plug is denser for stratified conditions than for homogenous conditions, which makes the ignition more stable, as shown in Fig. 8 (see Table 7).

4.3. Effect of spark timing

The performance of an SI engine depends on many factors, and spark timing is an important one. Spark timing in an SI engine is the timing of electric spark application to ignite the combustion chamber's air–fuel mixture. Exact spark timing is crucial to enhancing performance and controlling engine emissions. Establishing the correct spark time increases the efficiency and reduces emissions, allowing SI engines to comply with future emission standards (Gölcü et al., 2005).

Ji et al. (2010) experimented on a four-cylinder SI engine with hydrogen-enriched gasoline. According to the study, the indicated mean effective pressure (IMEP) first increased and then decreased with spark timing advancement for a given excess air ratio. IMEP is one of the key parameters influencing an engine's capability. Fig. 9 shows the variation of IMEP with spark timing based on two different excess air ratios and 3% hydrogen addition. The attainment of maximum IMEP spark time retards after hydrogen addition. This is because of the ease of combustion of hydrogen-enriched gasoline mixture, which can be explained by a wide flammability range and low hydrogen ignition energy. With further retardation between 24° and 32° CA BTDC for excess air ratios of 1.2 and 1.4, respectively, pure gasoline exhibited higher IMEP than a hydrogen–gasoline mixture. This is because the combustion of hydrogen-enriched gasoline completes earlier and produces negative compression work.

The flame development period (CA0–10) and flame propagation period (CA10–90) indicate the resulting mixture's combustion quality (Martinez et al., 2019; Salazar and Kaiser, 2011). For a given spark advance (Fig. 10(a) and (b)), both periods are reduced with hydrogen addition as the high burning speed of

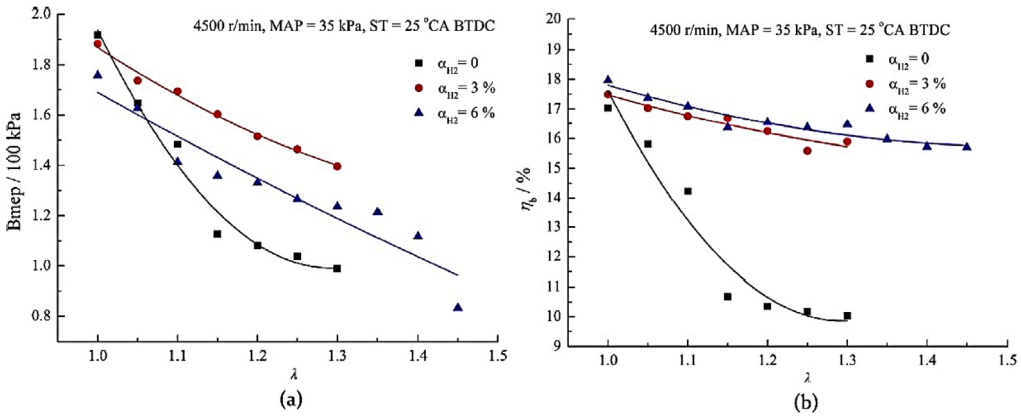

Fig. 6. Variation of (a) brake mean effective pressure (BMEP) and (b) brake thermal efficiency (BTE) with excess air ratio (λ) at partial load (Su et al., 2017c).

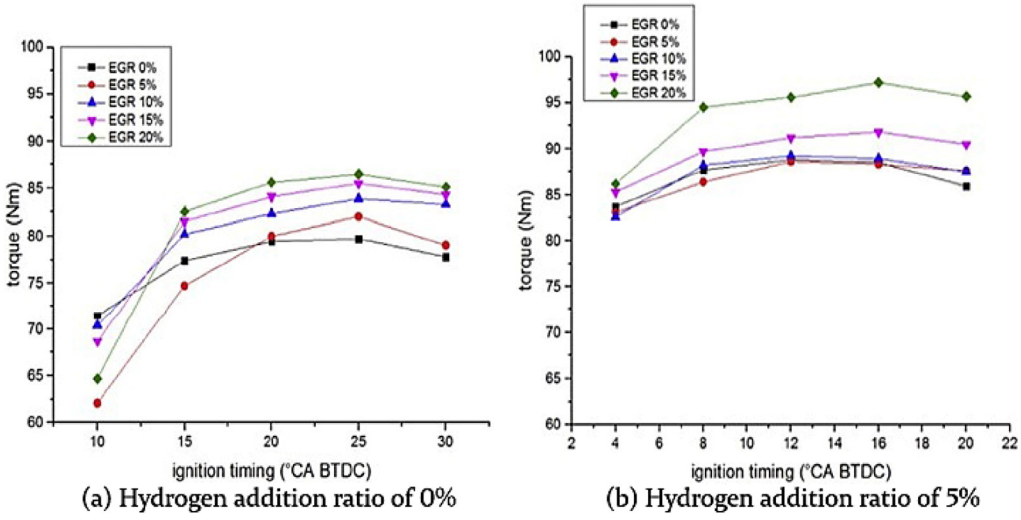

Fig. 7. Variation of torque with ignition timing with (a) 0% and (b) 5% hydrogen fractions (Du et al., 2017).

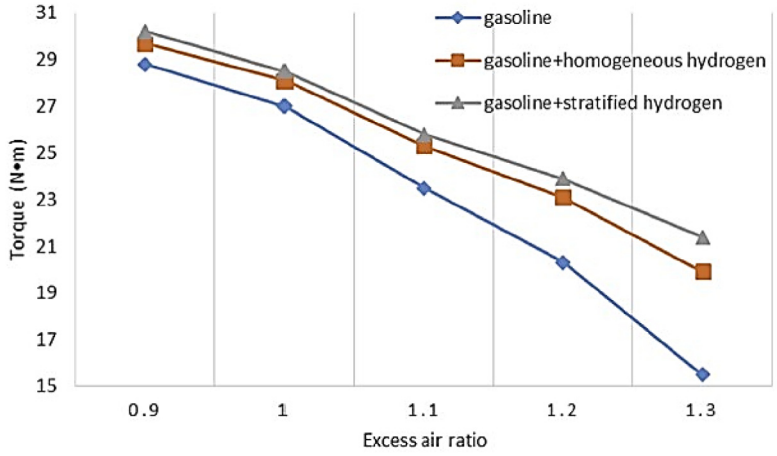

Fig. 8. Effects of hydrogen conditions on torque for various excess air ratios (Yu et al., 2019b).

hydrogen allows the resultant mixture to be easily ignited. CA0–10 is increased and CA10–90 is reduced with the retardation of spark timing. This indicates that the retardation of spark timing results in increased cylinder pressure and temperature at the start of combustion, which provides a better atmosphere for the fuel to ignite.

When using a mixture of fuels, the spark timing must be precise to improve performance. Elsemary et al. (2017) studied the effect of spark timing on a small SI engine fueled with hydrogen–gasoline mixtures with 0%, 24%, 28%, 29%, 31%, and 49% hydrogen volume fractions. It is noted from Fig. 11(a) that for given engine power and spark time, the specific fuel consumption (SFC)

Table 7
Summary of effects of engine torque and engine load.

References	Engine specification	Hydrogen induction system	Hydrogen fraction	Result
Ji et al, 2011. Ji and Wang (2011)	1.6 L, 4 stroke	PFI	3%, 5%, and 8%	• Increment in BTE and torque. • Reduction in exhaust losses.
Du et al, 2017. Du et al. (2017)	1.8 L, 4 stroke	DI	5% and 25%	• Enhancement in torque for same ignition timing and EGR flow rate. • 5% hydrogen was the best fraction for torque enhancement.
Su et al, 2017. Su et al. (2017c)	160 cc, rotary engine	PFI	3% and 6%	• Every hydrogen-enriched test fuel showed an increment in BMEP and thermal efficiency.
Yu et al, 2019. Yu et al. (2019b)	2.0 L, 4 stroke	DI	20%	• Enhancement in torque. • Stratified condition is superior to homogenous condition. • 0.55% and 3.3% increase for BTE and maximum pressure respectively for stratified condition.

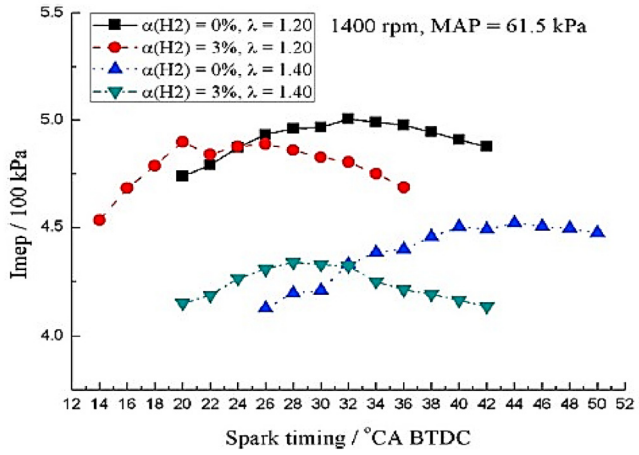

Fig. 9. Indicated mean effective pressure (IMEP) versus spark timing for two excess air ratios (λ) and hydrogen volume fractions (Ji et al., 2010).

reduces with hydrogen addition up to 31%. Beyond that, higher fuel consumption is observed because of the lack of air required to complete the combustion. Minimum fuel consumption was noted at 30° BTDC for all test fuels with hydrogen addition. This indicates that by moving the spark timing close to TDC, further reduction in SFC can be obtained. A similar trend was observed for BTE, where the optimum spark timing for hydrogen-added test fuels is 30° BTDC, as shown in Fig. 12(b). When the spark timing shifts to near TDC, improved combustion is obtained over a short time during the expansion stroke, leading to high heat generation resulting in higher BTE.

For a constant excess air–fuel ratio of 1.2 with hydrogen volume fractions of 0% to 10%, Shi et al. (2017) investigated the effect of spark timing on a hydrogen direct injection stratified gasoline engine. Fig. 12(a) shows the instantaneous heat release rate (HRR) variation for a 9% hydrogen volume fraction. It is observed that with spark angle advancement, the HRR increases, and the crank angle delays. It is observed that advancing the spark timing results in a late combustion process where the attainment of peak HRR is also delayed. Su et al. (2017a) also conducted experiments on spark timing effects for a rotary engine fueled by a hydrogen–gasoline mixture. According to the authors, HC, CO and NO_x emissions increased with the retardation of spark timing. Fig. 12(b) shows that the HC emissions decrease as the hydrogen fraction increases. The CO emissions also followed a similar trend, as shown in Fig. 14(a). In the case of HCs, a shorter quenching distance caused lower emissions, whereas the zero-carbon content of hydrogen promoted the reduction in CO emissions. However, NO_x emissions followed the opposite trend of the HC and CO emissions. Fig. 13(b) depicts the NO_x emission for different hydrogen volume fractions. An increase in hydrogen volume fraction increased NO_x emissions. This is because addition of more hydrogen created higher temperatures inside the cylinder, resulting in higher thermal NO_x.

The ignition timing is an important factor for determining the optimum performance for an engine. In a SI engine, ignition timing is the relative timing of the current position of the piston or crankshaft angle associated with the release of the spark towards the end of compression stroke. Yu et al. (2017) investigated the ignition timing effect on hydrogen addition in SI engine. Fig. 14(a) shows different hydrogen ignition timing for an injection pressure of 4 MPa. It was observed that Mean Effective Pressure (MEP) first increased and then decreased when the ignition time is delayed. For a delayed timing, MEP showed a little change and then reduces rapidly for further delay of ignition. Whereas for ignition advancement, the MEP showed significant change and the MEP difference between lower value and peak value was large.

For a higher hydrogen fraction, Du et al. (2017) studied the variation of engine torque against ignition timing for 25% hydrogen addition along with the EGR operation. As observed from Fig. 14(b), there is an initial increment in torque after which it reduces. When the ignition timing is delayed, the output torque was too low. The increment in the torque was not that significant for a higher hydrogen fraction when compared to a lower hydrogen fraction. But Hydrogen addition increased the peak torque from 79.9 Nm to 87.5 Nm from gasoline only operation to 25% hydrogen addition operation (see Table 8).

4.4. Effect of hydrogen–gasoline composition ratio

In a hydrogen–gasoline dual fuel engine, gasoline dependency can be reduced to a large extent by increasing the hydrogen fraction, but high hydrogen contributions increase the tendency toward engine knocking and backfiring because of hydrogen's low ignition energy (Szwaja et al., 2007). In addition, it has been noted that volumetric efficiency decreases with increasing hydrogen fraction, irrespective of the engine load. This is mainly because the hydrogen fuel takes up significant space, leaving less room for the incoming air (Geo et al., 2008).

Alcohols are also considered a promising alternative fuel in SI engines because they have properties similar to gasoline (Göktaş et al., 2021; Feng et al., 2019; Thakur et al., 2017). Many

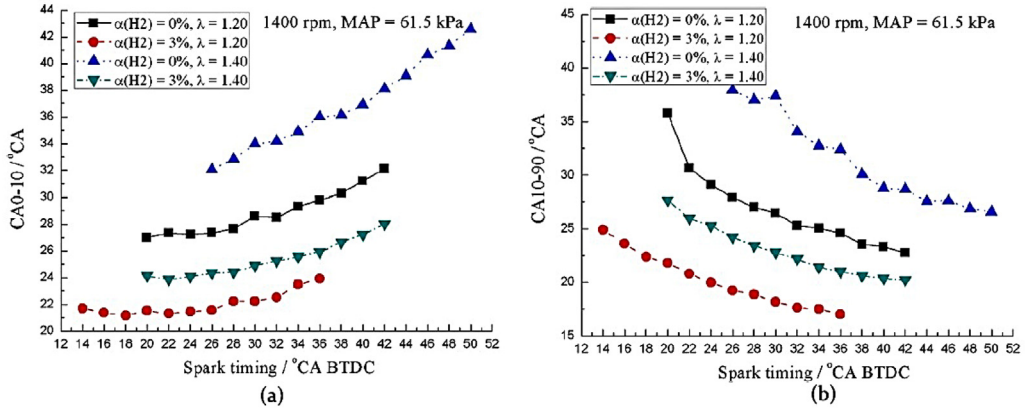

Fig. 10. (a) Flame development period (CA0–10) and (b) flame propagation period (CA10–90) versus spark timing for two excess air ratios (λ) and hydrogen volume fractions (Ji et al., 2010).

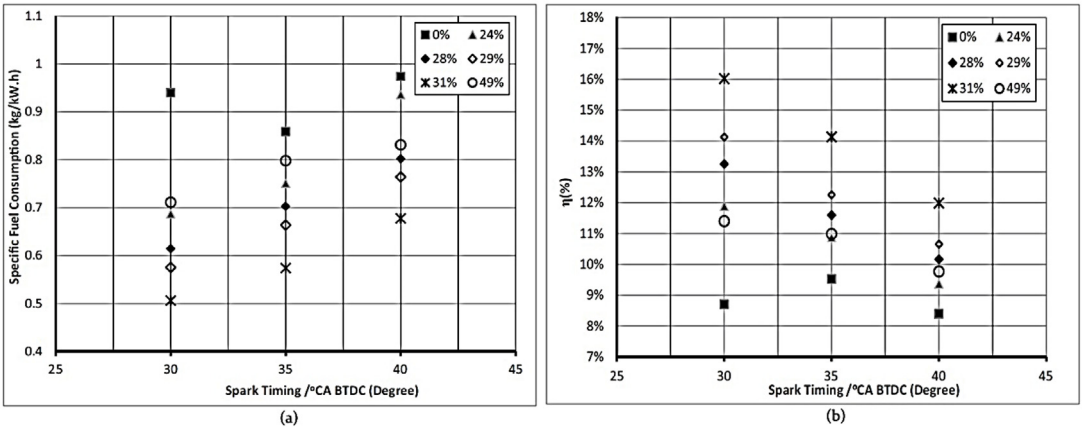

Fig. 11. Variation of (a) specific fuel consumption (SFC) and (b) brake thermal efficiency (BTE) with spark timing for different hydrogen fractions (Elsemary et al., 2017).

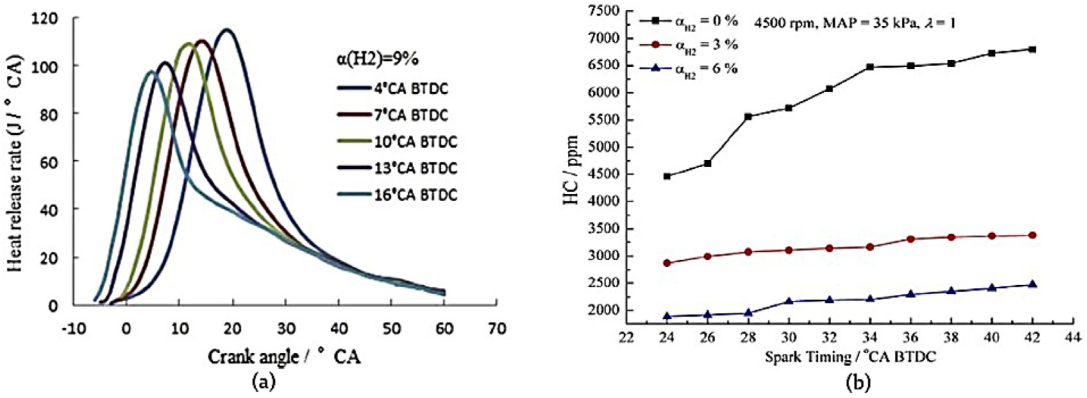

Fig. 12. (a) Heat release rate (HRR) versus crank angle (CA) at 9% hydrogen volume fraction for different spark timings (Shi et al., 2017); (b) Hydrocarbon (HC) emissions versus spark timing for different hydrogen fractions (Su et al., 2017a).

researchers have also discovered that the addition of hydrogen, even in trace amounts, can enhance SI engine performance because of its distinctive properties, claiming superior results to alcohol. Yang and Ji (2018) conducted a comparative study on the effects of hydrogen on gasoline and n-butanol in a rotary engine. The hydrogen volume fraction was raised from 0% to 5.12% for hydrogen–gasoline and from 0% to 6.3% for hydrogen–n-butanol mixtures. The results showed that with an increase in hydrogen volume fraction, BTE increased because of improved combustion, also resulting in a significant reduction in HC emissions, while the zero-carbon content of hydrogen promoted reduced CO and CO_2 emissions. These authors also reported that the flame development and flame propagation period were reduced with increased hydrogen volume fraction.

As mentioned earlier, the main drawbacks of using hydrogen are its propensity toward knocking and backfiring. Many studies have observed that these drawbacks can be addressed by adopting proper design parameters such as compression and equivalency ratios (Yip et al., 2019; Duan et al., 2014). The best approach for enhancing the efficiency of a SI engine fueled with

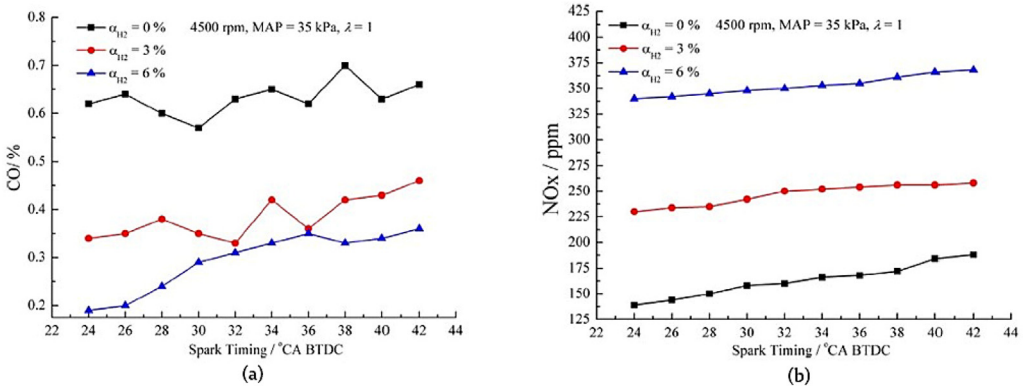

Fig. 13. (a) CO and (b) NO_x emissions versus spark timing for different hydrogen fractions (Su et al., 2017a).

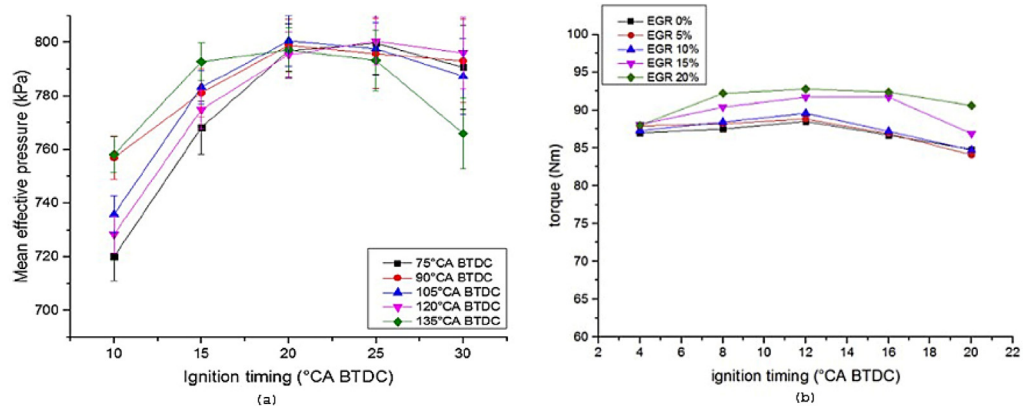

Fig. 14. (a) MEP against ignition timing for 10% hydrogen fraction (Yu et al., 2017) and (b) Torque against ignition timing for 25% hydrogen fraction (Du et al., 2017).

Table 8
Summary of the effects of spark timing.

References	Engine specification	Hydrogen induction system	Hydrogen fraction	Result
Ji et al, 2010. Ji et al. (2010)	1.6 L, 4 stroke	PFI	3%	• Spark timing retards after hydrogen addition. • Gasoline exhibited higher IMEP between 24° and 32° CA BTDC.
Elsemary et al, 2017. Elsemary et al. (2017)	389 cc, 4 stroke	PFI	24%, 28%, 29%, 31%, and 49%	• SFC increased beyond 31% hydrogen fraction. • SFC reduces when retarding spark time towards TDC.
Shi et al, 2017. Shi et al. (2017)	1.8 L, 4 stroke	DI	3%, 5%, 7%, 9%, and 10%	• HRR is increased and combustion is delayed with spark advancement.
Su et al, 2017. Su et al. (2017a)	160 cc, 4 stroke	PFI	3% and 6%	• Increase in HC, CO and NO_x emissions with spark time retardation.
Yu et al, 2017. Yu et al. (2017)	1.798 L, 4 stroke	DI	10%	• MEP decreased when ignition timing delayed. • For ignition advancement the difference between peak and lower value was large.
Du et al, 2017. Du et al. (2017)	1.8 L, 4 stroke	DI	5% and 25%	• Torque increased initially and then decreased. • Torque increment was not significant for higher hydrogen compared to low hydrogen fraction.

pure gasoline is to extend its lean burn characteristics, which would lead to misfire issues. This misfire issue can be mitigated either by improving the gasoline characteristics or introduce a gaseous fuel like hydrogen to extend the lean conditions (Salek et al., 2021; Vinoth Kanna and Paturu, 2020).

Du et al. (2016) conducted research on the effects of hydrogen fraction (0% to 11.9%) with hydrogen DI operating on lean burn characteristics. Fig. 15(a) shows the variation in combustion duration for different hydrogen fractions. For a given equivalence ratio, combustion duration shortens with the increase in hydrogen addition due to the rapid combustion properties of hydrogen. For equivalence ratios up to 1.5, the variation in combustion duration is not very pronounced but begins to expand significantly beyond this level. The effect of hydrogen enrichment on the

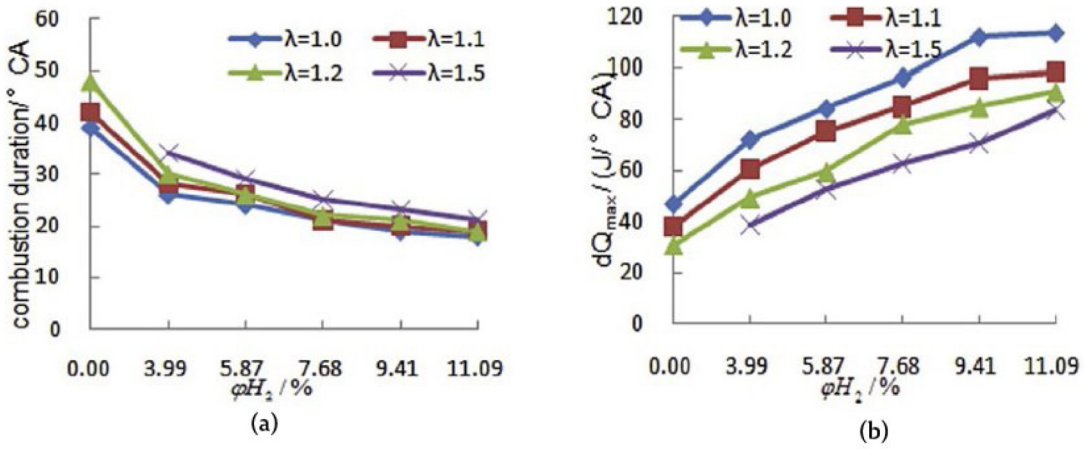

Fig. 15. Effect of hydrogen addition fraction on (a) combustion duration and (b) maximum heat release rate at different equivalence ratios (Du et al., 2016).

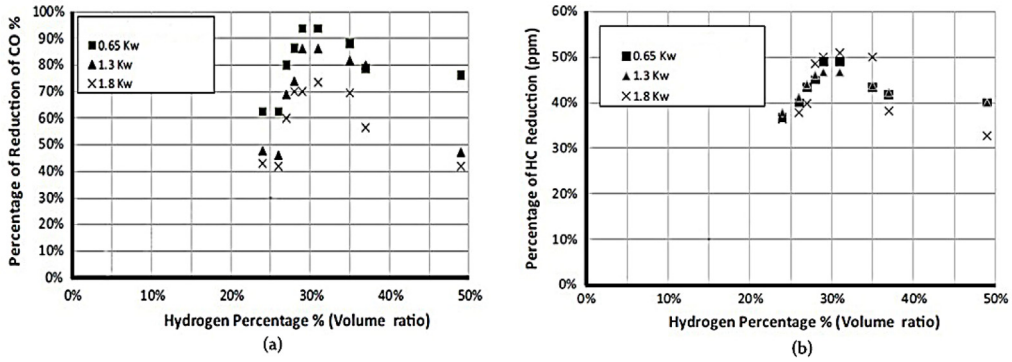

Fig. 16. Percentage (a) CO and (b) hydrocarbon (HC) reduction with hydrogen volume ratio (Elsemary et al., 2016).

maximum heat release rate is shown in Fig. 15(b). The maximum heat release rate increases with increasing hydrogen fraction and decreases with increasing equivalence ratio. The rapid diffusivity of hydrogen in the incoming air and enhanced flame propagation increases the maximum heat release rate with a corresponding increase in hydrogen fraction. The combustion duration expands, and the degree of constant volume combustion decreases with an increase in equivalence ratio, reducing the maximum heat release rate.

Elsemary et al. (2016) investigated the performance of an SI engine fueled with hydrogen–gasoline mixtures with high hydrogen volume fractions. The hydrogen introduced to the intake manifold was 24% to 49% of the total intake volume. The results showed an enhancement in thermal efficiency, and hydrogen addition led to higher cylinder pressures. Fig. 16(a) and (b) show the reduction in CO and HC emissions as a function of brake power for different hydrogen volume ratios. For a given power, the presence of CO in the exhaust declines with increased hydrogen fraction to 31%, beyond which higher emissions result from a low energy flow rate and low-temperature incomplete combustion. The HC emissions also followed a similar trend to the CO emissions. The initial reduction up to 31% hydrogen volume fraction was because of high flame velocity and the high temperature of the hydrogen–gasoline mixture, which promoted combustion.

The flame propagation information is used to determine engine stability and thermal efficiency. Ji et al. (2013) has investigated the variation of flame propagation speed by varying the crank angle under different hydrogen volume fraction. In author's work the flame propagation period was calculated from 10° CA after the spark discharge till 80% mass of fuel is burned. From Fig. 17(a) it was observed that increase in hydrogen volume fraction increases the flame propagation speed and advances the crank angle. The flame propagation speed for 3% and 6% hydrogen volume fraction was 15.20 m/s at 6.4° CA and 17.78 m/s at 2.8° CA respectively, whereas for gasoline only operation it was 11.08 m/s at 11.7° CA. After reaching the peak value, the propagation speed is gradually reduced due to the dilution of fuel–air mixture with the increased concentration of combustion products.

To obtain better performance and to use hydrogen in a better way, hydrogen injection is divided into stages. Li et al. (2020) investigate the effect of first injection of hydrogen on engine operating on hydrogen/gasoline blend. Hydrogen proportion injected firstly out of all hydrogen injected in both injections. The total hydrogen fraction for both injection was 20%. Fig. 17(b) shows the variation of first injection against the HRR. The HRR was more intense and advanced than the gasoline with hydrogen addition. The authors varied the first injection proportion as 25%, 33%, 50%, 67% and 75%. It was observed that at first injection proportion of 33%, the combustion and ignition rate reached the peak value. For further increase in first injection proportion the hydrogen injection happened early, where the hydrogen mixture became too homogenous which find difficulty to fasten up the ignition (see Table 9).

4.5. Effect of excess air ratio

The excess air ratio is an important factor for performance tuning and is an anti-pollution parameter for an SI engine. The amount of oxygen required must be specified accurately for precise excess air calculations because the excess air ratio depends

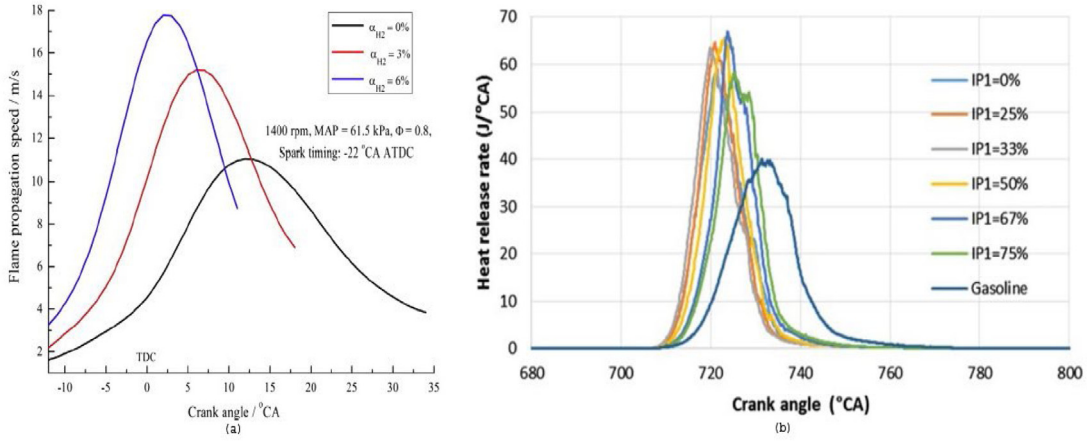

Fig. 17. (a) Variation of flame propagation speed against crank angle under different hydrogen volume fraction (Ji et al., 2013) and (b) Variation of HRR against the Crank angle for different first injection proportion of hydrogen (Li et al., 2020).

Table 9
Summary of the effects of hydrogen–gasoline composition ratio.

References	Engine specification	Hydrogen induction system	Hydrogen fraction	Result
Elsemary et al, 2016. Elsemary et al. (2016)	389 cc, 4 stroke	PFI	24%, 26%, 27%, 28%, 29%, 31%, 35%, 37%, and 49%	• Increase in thermal efficiency. • Reduction in CO and HC emission.
Yang et al, 2018. Yang and Ji (2018)	160 cc, rotary engine	PFI	0 to 5.2%	• Increase in BTE. • Reduction in flame development and flame propagation period.
Du et al, 2016. Du et al. (2016)	1.8 L, 4 stroke	DI	3.99%, 5.87%, 7.68%, 9.41%, and 11.09%	• Reduction in combustion duration. • Increase in HRR.
Ji et al, 2013. Ji et al. (2013)	1.6L, 4 stroke	PFI	3% and 6%	• Hydrogen addition increases the flame propagation speed. • After reaching peak value, it then decreases due to increased concentration of combustion products.
Li et al Li et al. (2020)	1.984L, 4stroke	DI	20%	• Split injection enhanced the combustion rate. • Best first injection proportion was find out to be 33%.

on the engine specification, fuel used, and atmospheric conditions.

Liang (2019) investigated the effect of excess air ratio and hydrogen fraction in hydrogen DI gasoline engines. The experimental trials consisted of three excess air ratios (1, 1.2, and 1.5) and four hydrogen fractions (5.3%, 7.2%, 8.9%, and 10.5%). The cylinder pressure curves provide valuable information regarding the combustion behavior. Fig. 18(a) and (b) show the variation of in-cylinder pressure and heat release rate as a function of the crank rotation measurement for the different excess air ratios. As the excess air ratio increases, the value of the peak in-cylinder pressure and HRR reduces because the hydrogen–gasoline mixture becomes leaner with increased excess air ratio. Therefore, the combustion rate depletes, and the combustion temperature decreases, resulting in incomplete combustion. It is also seen from Fig. 19(a) that the exhaust temperature decreases as the excess air ratio increases. When the excess air ratio increases from 1 to 1.2, the exhaust temperature first increases and then continuously decreases. This is because the oxygen ratio present in the cylinder increases initially, leading to better combustion where the exhaust temperature rises slowly. When the excess air ratio is larger than 1.2, the mixture gets leaner, reducing the combustion heat.

A similar trend in the engine emission characteristics to that of the exhaust temperature discussed above was observed in the study conducted by Niu et al. (2016). Fig. 19(b), 20(a), and 20(b) show the variation of HC, CO and NO_x emissions versus excess air ratio (1.0 to 2.1) for various hydrogen fractions. The HC emissions initially decreased and then increased with increasing excess air ratio, whereas the NO_x emissions showed the opposite trend. This is because of the enhanced combustion up to an excess air ratio of 1.2, beyond which the fuel mixture becomes leaner, reducing the oxygen ratio and cylinder temperature and leading to incomplete combustion. Because hydrogen has no carbon content, the CO emissions decreased from the stoichiometric condition up to an excess air ratio of 1.2, beyond which no noticeable difference was seen.

In the same work (Niu et al., 2016), the authors also examined the effect of excess air ratio on the flame development period and combustion duration for different hydrogen fractions. From Fig. 21, both periods were shortened with the hydrogen addition but expanded with increasing excess air ratio. It is noted that further increments in the hydrogen fraction reduce the negative effects of increasing excess air ratio, leading to rapid combustion, which is significant for enhancing engine efficiency. In contrast to the hydrogen direct injection, Ji and Wang (2011) investigated the combustion analysis (flame development period and combustion duration) for engine running at 800 rpm using hydrogen PFI system. Authors also observed the prolongation in combustion periods with increase in excess air ratio. This observation

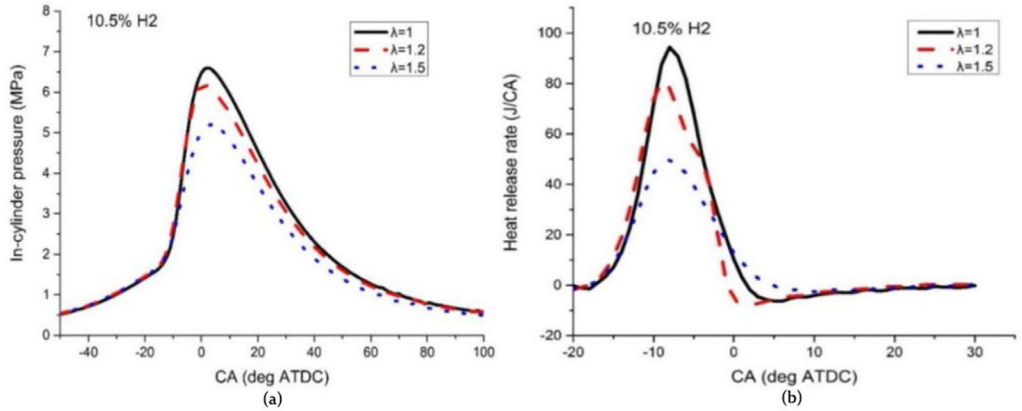

Fig. 18. Variation of (a) in-cylinder pressure and (b) heat release rate (HRR) with crank angle (CA) at different excess air ratios (Liang, 2019).

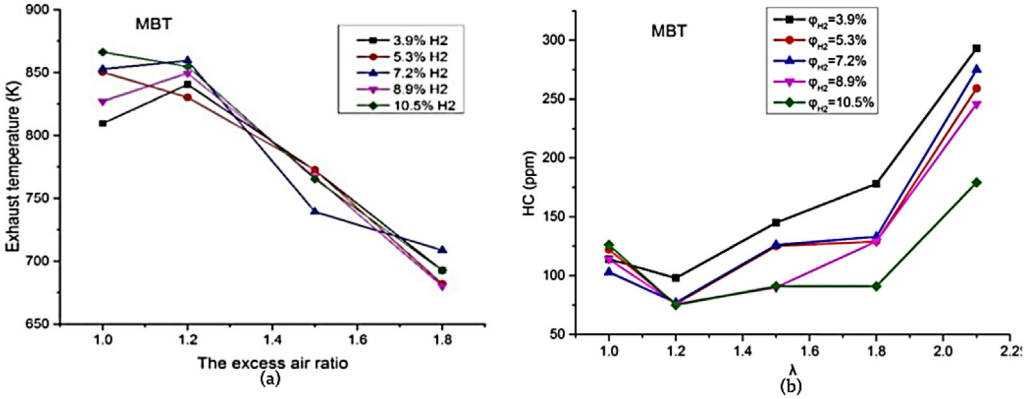

Fig. 19. Variation of (a) exhaust temperature (Liang, 2019) and (b) HC emission (Niu et al., 2016) with excess air ratio for different hydrogen fractions.

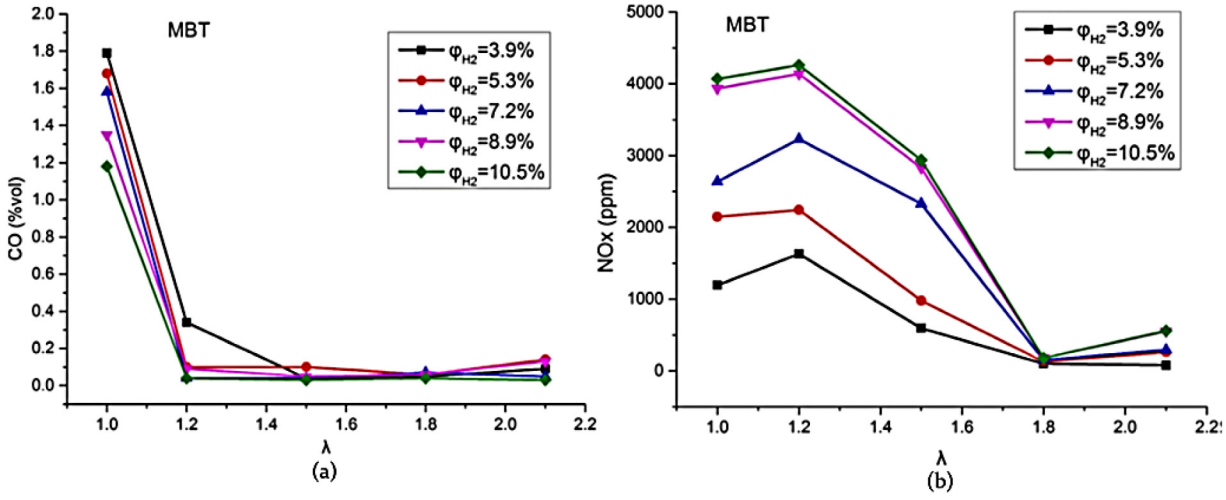

Fig. 20. Variation of (a) CO and (b) NO_x emission with excess air ratio for different hydrogen fractions (Niu et al., 2016).

was mainly due to the wide flammability limit and low ignition energy of hydrogen.

Studies concerning nanoparticle emissions from engines are growing because of increasing evidence that the toxicity increases with a reduction in particle size (Sahu and Hayes, 2017; Sharifi et al., 2012). Sun et al. (2016) investigated the effect of hydrogen injection on particle emission under lean conditions ($\lambda = 1.2$, 1.3, and 1.4). Fig. 22 shows the variation in the number of particles for 12% hydrogen fraction for different excess air ratios. It is noted that with an increase in excess air ratio, the total number of particles decreased. This decrease was mainly noted for nucleation mode particles. The authors concluded that accumulation mode particles under ultra-lean combustion are not affected by either ignition timing or hydrogen fraction. When the engine runs on lean condition, the higher hydrogen fraction will drastically reduce the carbon concentration and will also affect the soot

Table 10
Summary of excess air ratio effect studies.

References	Engine specification	Hydrogen induction system	Hydrogen fraction	Result
Sun et al, 2016. Sun et al. (2016)	1.8 L, 4 stroke	DI	4%, 8%, and 12%	• Total number of particles decreases with increasing excess air ratio.
Niu et al, 2016. Niu et al. (2016)	1.8 L, 4 stroke	DI	3.9%, 5.3%, 7.2%, 8.9%, and 10.5%	• HC emission increased with increasing excess air ratio. • NO_x emission decreased with increasing excess air ratio.
Liang et al, 2019. Liang (2019)	1.8 L, 4 stroke	DI	3.9%, 5.3%, 7.2%, 8.9%, and 10.5%	• Peak in-cylinder pressure and HRR decline as excess air ratio increases.
Ji et al, 2011 Ji and Wang (2011)	1.6 L, 4 stroke	PFI	3%, 5%, and 8%	• Flame development and combustion duration period increased with increase in excess air ratio.

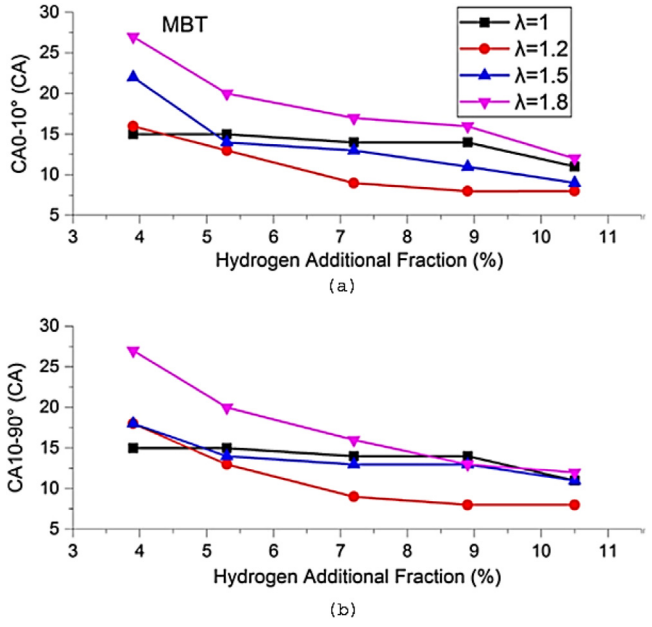

Fig. 21. (a) Flame development duration (CA0–10) and (b) Flame propagation duration (CA10–90) versus hydrogen fraction for different excess air ratios (Niu et al., 2016).

formation process, which results in less nucleation mode (see Table 10).

4.6. Effect of EGR flow rate

EGR is a system used to direct a portion of the exhaust gas back to the combustion chamber. The introduction of EGR into IC engines delays the combustion process to reduce NO_x emissions. The optimum operation of the EGR throttle valve can reduce NO_x emissions to half that of engines without EGR. The EGR flow rate is crucial because greater EGR gas flows slow down the combustion rate, leading to instability. Therefore, using EGR with optimized parameters could enhance efficiency with reduced emissions. It has been reported in the literature that increases in both EGR and hydrogen fraction have resulted in enhanced BMEP and ITE with considerable NO_x emission reductions (Yu et al., 2019a; Kim et al., 2017).

Yu et al. (2019a) studied the EGR effect on a lean burn naturally aspirated SI engine fueled with a hydrogen–gasoline mixture for different excess air ratios of 1.0, 1.2, and 1.4. Here, only the variation of different parameters at an excess air–fuel ratio of 1.2 is discussed, as it is considered the optimum condition in many works (Niu et al., 2016; Liang, 2019). Fig. 23(a) shows the contrast between BMEP and hydrogen fraction at different EGR flow rates. It is observed that with an increment in the hydrogen fraction, the BMEP increases at a given EGR flow rate. An initial increment was observed for hydrogen fractions of 0% and 5% because of the reduction in pumping losses as the throttle opening increases the EGR flow rate. Further increases in the EGR flow rate negatively affect the combustion process, but when the hydrogen fraction increases beyond 15%, this negative effect is overcome by the hydrogen's rapid flame speed, increasing BMEP.

EGR is a system that mainly addresses engine emissions. Fig. 23(b) represents the variation in NO_x emissions. It is evident that an increase in hydrogen fraction increases NO_x emissions, but EGR reduces NO_x with increasing EGR flow rate. The emission of HCs and CO as a function of EGR flow rate is shown in Fig. 24(a)–(b). An increase in hydrogen fraction reduces HC emissions because of better combustion but was negatively affected by an increase in EGR flow rate leading to combustion instability. The CO emission also showed a similar trend to the HC emissions, increasing with EGR flow rate and decreasing with higher hydrogen fraction. Because hydrogen does not add to the carbon content, CO emissions decline with hydrogen addition, whereas the increase in CO emissions with increasing EGR flow rate is due to an increase in specific heat capacity, which reduces the in-cylinder temperature so that CO is not completely oxidized to CO_2.

For a turbocharged SI engine, Kim et al. (2017) investigated the effect of hydrogen addition on combustion and emissions with EGR for three hydrogen fractions (1%, 3%, and 5%). Fig. 25(a) shows the variation of indicated thermal efficiency versus EGR flow rate at BMEPs of 4, 6, and 8 bar for a 5% hydrogen fraction. Hydrogen enrichment improved ITE for all operating conditions because hydrogen made the fuel mixture more ignitable, reducing the combustion duration. The EGR flow rate initially improved the ITE, followed by a decrease due to increased combustion instability which is more pronounced at 4 and 6 bars. Apart from that, as the BMEP increases corresponding increase in ITE was noted for both gasoline only and hydrogen enrichment operation. For BMEP of 8 bar, after 25% EGR dilution there was not much increase or reduction in ITE, which shows a great stability was achieved. The heat release and flame behavior details are shown in Fig. 25(b). The effect of hydrogen enrichment on the combustion duration increased with increasing EGR flow rate. The effect of hydrogen was more pronounced on flame development (CA0–10) than on flame propagation (CA10–90). A deviation from the normal trend was observed for CA10–90 at 8 bar BMEP with a 20% EGR flow rate and was attributed to the hydrogen enrichment affecting the laminar flame speed mainly during initial combustion. Whereas CA10-90 was reduced for BMEP's of 4 and 6 bar.

In the past few years, researchers have turned their attention toward the reliability of alternate fuels and enhancing engine efficiency and burning qualities to overcome the emission issues

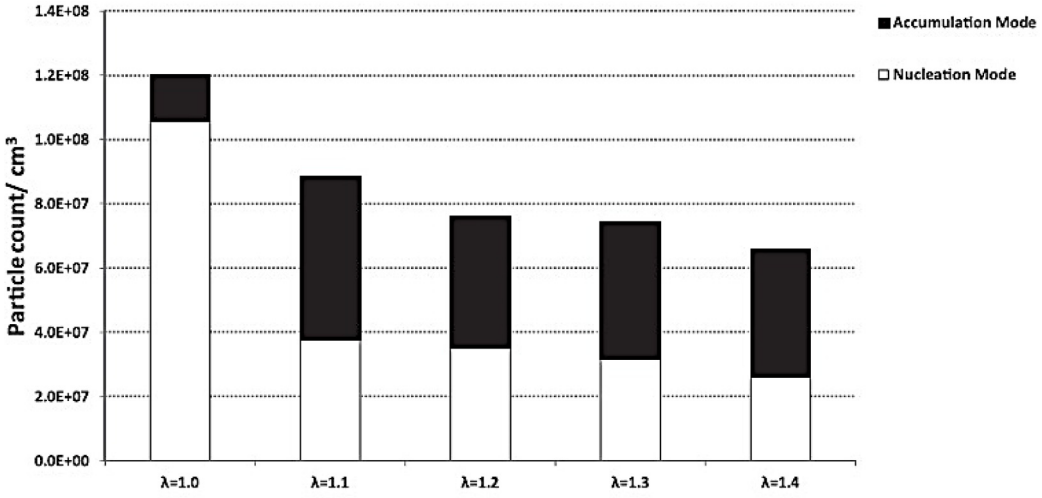

Fig. 22. Number of particles versus excess air ratio (λ) for a 12% hydrogen fraction (Sun et al., 2016).

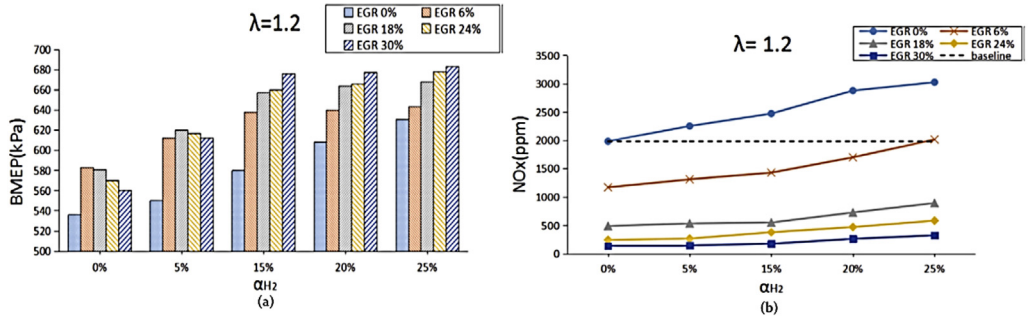

Fig. 23. Variations of (a) BMEP and (b) NO_x emissions for different hydrogen fractions and EGR flow rates (Yu et al., 2019a).

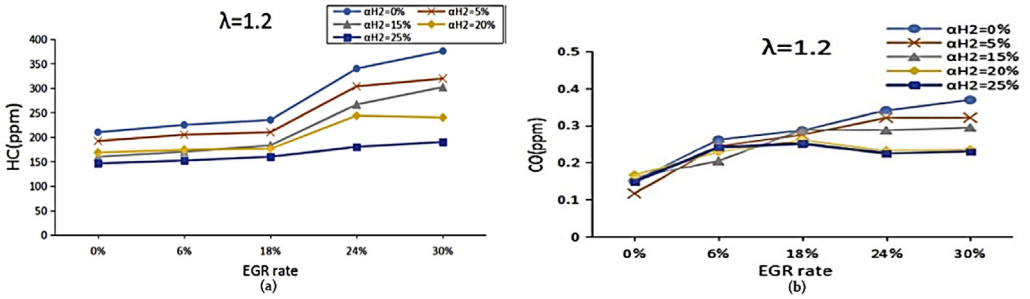

Fig. 24. Variations of (a) HC and (b) CO emissions for different hydrogen fractions and EGR flow rates (Yu et al., 2019a).

of conventional IC engines by using nanoparticles in fuel mixtures (Elwardany et al., 2021; Taghavifar et al., 2020; Amirabedi et al., 2019). Manigandan et al. (2019) investigated the effect of TiO_2 nanoparticles in an SI engine fueled with a hydrogen–gasoline mixture operating with EGR. The tests were performed using different hydrogen fractions (5%, 10%, and 25%), EGR flow rates (5%, 10%, and 20%) and 5% TiO_2 nanoparticles. Fig. 26(a) and (b) show the variation of torque and cylinder temperature with ignition timing for different EGR flow rates and a 5% hydrogen fraction. It is evident that torque increases as ignition timing increases to 25° BTDC. In addition, 13% and 2.5% improvements in torque were observed for a 20% EGR flow rate and 5% TiO_2 particles, respectively. The improvement was most pronounced at higher hydrogen fractions and high EGR flow rates. The throttle opening is increased at higher flow rates, which reduces throttle losses, leading to higher torque and efficiency. The main objective of EGR is to quench the combustion chamber. As the EGR flow rate increases, the cylinder temperature reduces drastically irrespective of ignition timing because EGR absorbs heat, reducing the combustion temperature. The addition of TiO_2 nanoparticles (T-EGR) increased the cylinder temperature, which improved the combustion stability leading to improved heat release and increased temperature (see Table 11).

4.7. Effect of hydrogen addition on cyclic variation

Cyclic variations, or cycle-to-cycle variation (CCV), are directly linked to vehicle drivability. CCV studies have been reported in recent literature on SI, CI, and homogeneous charge compression ignition (HCCI) engines (Yang et al., 2021; Li et al., 2017; Kaleli et al., 2015). CCV can potentially deteriorate the engine's output torque, resulting in combustion instability, undesirable engine noise, and vibration. Various sources of cyclic variation in a SI engine have been reported in many publications, such as: (a)

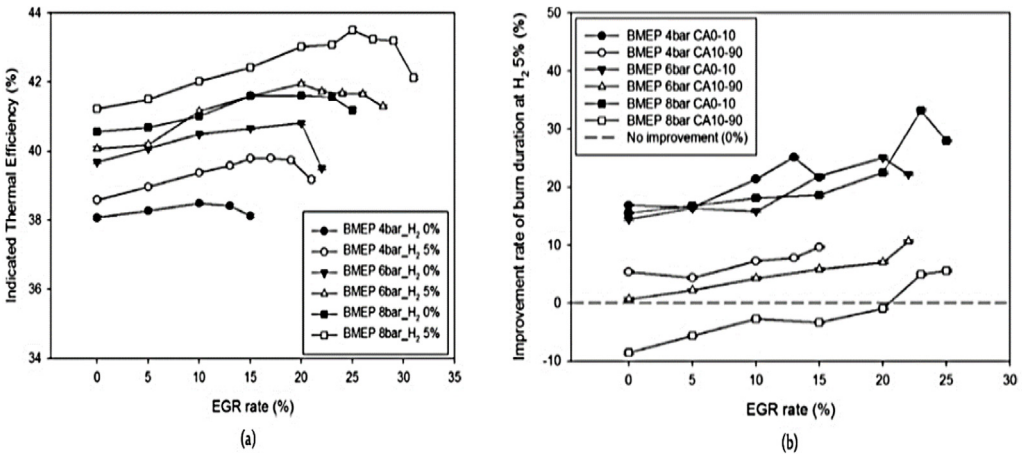

Fig. 25. Variations of (a) ITE and (b) CA0-10 and CA10-90 improvement versus EGR flow rate for different hydrogen fractions (Kim et al., 2017).

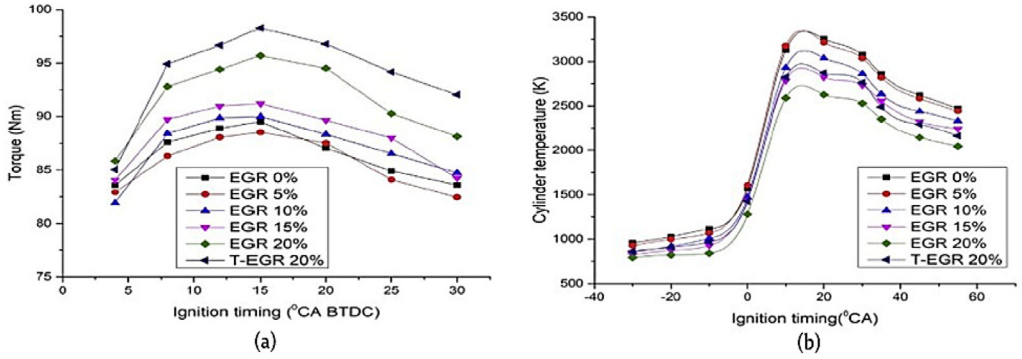

Fig. 26. Variations of (a) torque and (b) cylinder temperature versus ignition timing with a 5% hydrogen fraction (Manigandan et al., 2019).

Table 11
Summary of the effects of EGR flow rate.

References	Engine specification	Hydrogen induction system	Hydrogen fraction	EGR Flowrate	Result
Yu et al, 2019. Yu et al. (2019a)	1.8 L, 4 stroke	DI	5%, 15%, 20%, and 25%	6%, 18%, 24% and 30%	• Hydrogen addition enhanced the negative effect of EGR on combustion. • NO_x emission reduces with an increase in EGR flow.
Kim et al, 2017. Kim et al. (2017)	2.0 L, 4 stroke	PFI (intercooler inlet)	1%, 3%, and 5%	0% to 30%	• ITE increased initially and decreased due to EGR instability.
Manigandan et al, 2019. Manigandan et al. (2019)	2.0 L, 4 stroke	DI	5%, 10%, and 25%	5%, 10%, and 20%	• Increase in torque and efficiency as hydrogen fraction and EGR ratio increased.

turbulence formation in the cylinder flow field; (b) variation in fuel–air ratios; (c) the homogenous nature of fuel mixtures; (d) characteristics of spark discharge and flame development; (e) the quantity of leftover and recirculated exhaust gases in the cylinder (Ji et al., 2018; Beretta et al., 1983). The presence of high turbulence flow causes random time-dependent and spatial fluctuations in the variables that are associated with mixture formation which affects the fuel concentration in the cylinder. Apart from that, the lower fuel–air ratio than the desired ratio for optimum operation slows down the flame propagation process which mainly occurs during the initial flame development stage which results in the cyclic dispersion during combustion. In SI engines only few cycles are obtained at optimum spark timing (Galloni, 2009). Faster combustion cycles have advanced spark timing and slow combustion cycle has late spark timing. This fluctuations in spark timing also give rise to cyclic variation. Mostly the air–fuel mixture within the cylinder is not homogenously mixed with the recirculated exhaust gas, which affects the combustion process at time of spark. The burning velocity of hydrogen is much higher than that of gasoline, which may help in the reduction of cyclic variation (Wang and Ji, 2012). Apart from that, controlling the spark timing, defining correct air/fuel ratio, use of fuel with high RON are the few methods to reduce the cyclic variation (Kaleli et al., 2015; Chen et al., 2022; Ikeda and Kawahara, 2022). The extensively used method to evaluate cyclic variation is the coefficient of variation (COV) of IMEP. The COV is defined as

$$COV_x = \frac{\sigma_x}{\overline{X}} * 100\% \tag{7}$$

$$\sigma_x = \sqrt{\frac{\sum_{i=1}^{N}(X_i - \overline{X})^2}{N}} \tag{8}$$

$$\overline{X} = \frac{1}{N}\sum_{i=1}^{N} X_i \tag{9}$$

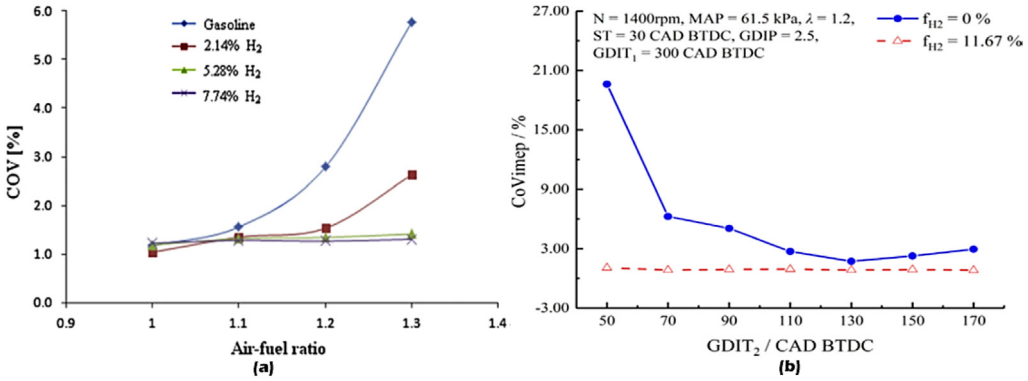

Fig. 27. (a) COV versus air–fuel ratio for different hydrogen fractions (Ceviz et al., 2012); (b) COV of IMEP with second gasoline DI (Ji et al., 2018).

where σ_x is the standard deviation of x, $\overline{X}$ is the mean value of a parameter for a specific combustion cycle, N is the number of test sample cycles and X_i is the selected combustion parameter such as IMEP, P_{max}, maximum pressure rise rate. It was found out to be that the drivability problems of vehicle usually shows up when the COV of IMEP exceeds 10% for a SI engine (Heywood, 2018).

To determine the relationship between the selected combustion parameter, the correlation coefficient (R) is obtained as

$$R(X, Y) = \frac{\frac{1}{n}\sum_i^n (X_i - \overline{X})(Y_i - \overline{Y})}{\sigma_X \sigma_Y} \quad (10)$$

Ceviz et al. (2012) investigated cyclic variation for an SI engine fueled with a gasoline–hydrogen blend under lean burn conditions. Fig. 27(a) indicates the influence of air–fuel ratio versus COV of IMEP for different hydrogen fractions of 2.14%, 5.28%, and 7.24%. This figure shows that an increased air–fuel ratio increased the COV and is more pronounced at air–fuel ratios beyond 1.1, indicating that cyclic variations increase when fuel mixtures become leaner. An increase in the hydrogen fraction reduces the COV, and the minimum COV was observed for the highest hydrogen fraction. This trend is confirmed by comparing the COV for different hydrogen fractions at air–fuel ratios of 1.0, 1.1, 1.2, and 1.3. The COV is nearly unchanged for hydrogen fractions beyond 5.28%, regardless of the air–fuel ratio. The authors concluded that hydrogen addition reduces the air–fuel ratio and cyclic variation dependency.

Similarly, Ji et al. (2018) conducted an experiment using hydrogen-blended gasoline injection with second gasoline DI to investigate the CCV of IMEP. Fig. 27(b) shows the variation of COV_{IMEP} against second gasoline DI ($GDIT_2$) for a hydrogen fraction of 11.67%. For pure gasoline, COV_{IMEP} initially has a slight deviation and significantly increases when $GDIT_2$ retards from 170° to 50° CA BTDC. But with hydrogen addition, the maximum COV was 1.07% compared with 20% for pure gasoline. The improvement in combustion stability was from the wide flammability limit, low ignition energy, and rapid flame velocity of hydrogen. Fuel combustion is one of the most important processes affecting engine performance, exhaust emission formation, and drivability (Tesfa et al., 2013). The addition of hydrogen affects the combustion characteristics because of variations in the air–fuel mixture formation. Niu et al. (2016) investigated the effect of hydrogen DI on combustion stability under a wide range of conditions. From Fig. 28, it is clear that for hydrogen fractions below 5.3%, the COV declines steadily from 3.3% to 0.51%, with the excess air–fuel ratio decreasing from 1.8 to 1. An increase in the hydrogen fraction reduces the COV for a given excess air ratio. Also, a slight COV increase was observed with an increase in hydrogen fraction at stoichiometric conditions. This was due

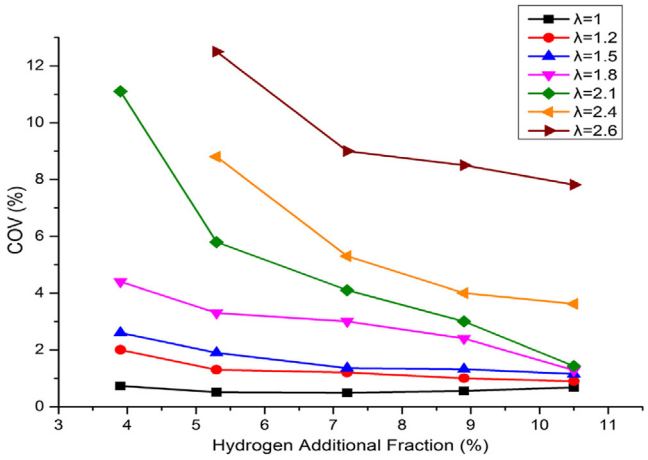

Fig. 28. COV versus hydrogen additional fraction for different excess air ratios (Niu et al., 2016).

to the high hydrogen concentration at the top of combustion chamber leaving a lean mixture in the remaining space, which negatively affects combustion stability.

Yu et al. (2016) conducted research on CCV with hydrogen DI under lean burn conditions. Fig. 29(a) and (b) show the CCV of maximum cylinder pressure versus combustion cycle number with a 15% throttle opening and a 10% hydrogen fraction. An increase in excess air ratio decreased the mean value of the maximum cylinder pressure and increased the CCV. As the excess air ratio increases, the mixture becomes leaner, deteriorating the flame propagation speed and long combustion duration, reducing maximum cylinder pressure, and increasing the CCV. The same trend was observed for the maximum pressure rise rate, as depicted in Fig. 30(a) and (b). However, the addition of hydrogen reduced the cyclic variation of the combustion period (see Table 12).

5. Future of hydrogen and NO_X control

The unique characteristics of hydrogen compared to other fuels used in SI engine makes it a promising approach, but still a challenging aspects for SI engine use. The properties like wide flammability, rapid flame travel and low ignition energy, make hydrogen a suitable fuel and is also responsible for abnormal combustion like preignition and backfire. In terms of eliminating backfire, the direct injection strategy for hydrogen into combustion chamber seems much more successful. But to combine the effect of PFI and DI, hydrogen direct injection and gasoline port

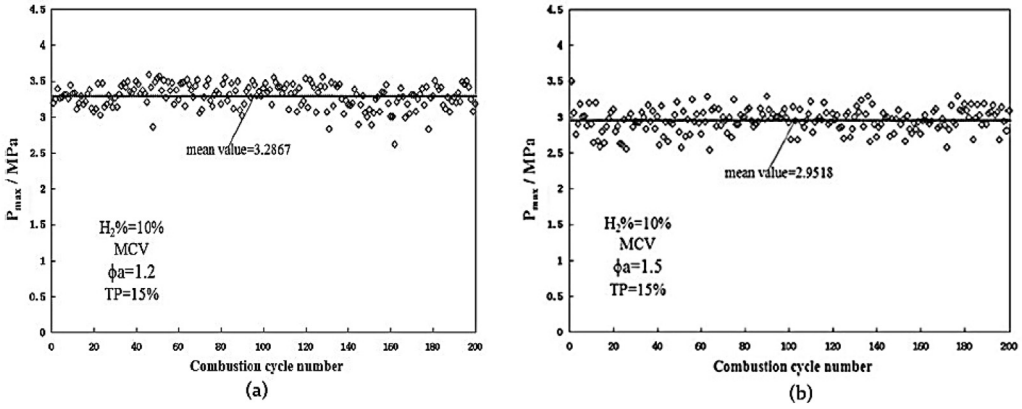

Fig. 29. Cycle-to-cycle variation (CCV) of maximum cylinder pressure at excess ratios of (a) 1.2 and (b) 1.5 for 10% hydrogen fraction (Yu et al., 2016).

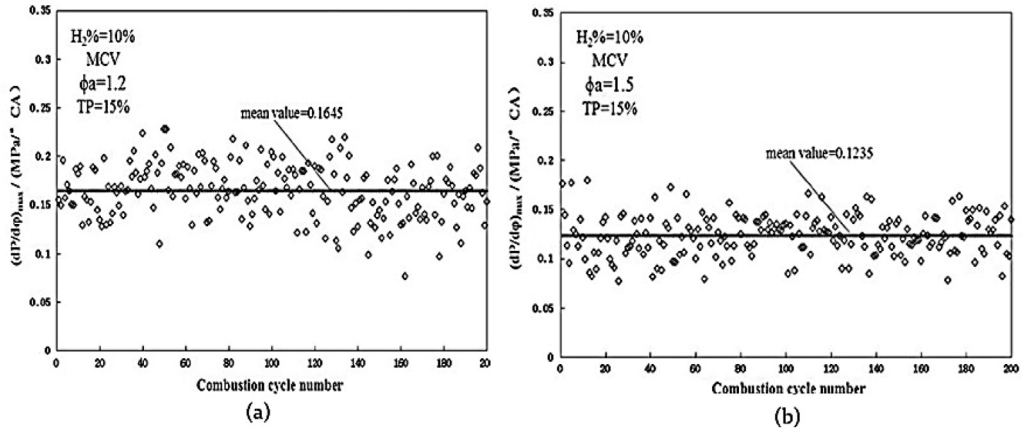

Fig. 30. Cycle-to-cycle variation (CCV) of maximum pressure rise rate at excess ratios of (a) 1.2 and (b) 1.5 for 10% hydrogen fraction (Yu et al., 2016).

Table 12
Summary of the effects of hydrogen addition on cyclic variation.

References	Engine specification	Hydrogen induction system	Hydrogen fraction	Result
Niu et al, 2016. Niu et al. (2016)	1.8 L, 4 stroke	DI	3.9%, 5.3%, 7.2%, 8.9% and 10.5%	• Increase in COV at stoichiometric conditions. • Hydrogen fractions up to 5.3% COV declined steadily.
Yu et al, 2016. Yu et al. (2016)	1.8 L, 4 stroke	DI	10%	• Increase in excess air ratio increases the CCV.
Ji et al, 2018. Ji et al. (2018)	1.6 L, 4 stroke	PFI	11.67%	• COV declined steadily from 20% to 1.07% with hydrogen addition.
Ceviz et al, 2012. Ceviz et al. (2012)	2.0 L, 4 stroke	PFI	2.14%, 5.28% and 7.24%	• Lean combustion increases the COV. • COV remains unchanged beyond a hydrogen fraction of 5.28%.

injection can be incorporated. The past work focused on building the hydrogen economy which has provided the building stone in the development of hydrogen fuel in SI engine. According to the above sections, Hydrogen enrichment has resulted in increased output and reduced the dependency on conventional gasoline. This hydrogen–gasoline dual fuel concept will provide a better alternate approach for the current SI engine. But still there are many unexposed areas which require further investigation to turn hydrogen fuel into an option for automobiles. But recent works have shown satisfactory result to use hydrogen along with gasoline to obtain better performance with reduced emission.

According to the reference cited throughout, indicates that NO_X emission is one of the major problem in using hydrogen in SI engine. Higher emission of NO_X is due to high combustion temperature, which is mainly caused when the engine is running on or near the stoichiometric conditions. Apart from that mixture homogeneity and spark timing also effects the NO_X formation.

To mitigate NO_X for a hydrogen fueled engine, lean burn operation is an excellent strategy. An equivalence ratio of 0.4 to 0.6 is optimal for an engine running on low to medium load. Das (1991) has investigated on the NO_X emission for hydrogen fueled SI engine and reported that for an equivalence ratio of 0.6, the NO_X level is too low for causing any environmental problems. But for an engine operating on an equivalence ratio below 0.4, may lead to misfiring which further increases NO_X emission.

Another way for controlling NO_X emission is by employing EGR. The recirculated exhaust gas quenches and brings down the combustion chamber temperature. This strategy also can reduce

the heat loss acquired through the wall of combustion chamber, which results in increased thermal efficiency. Apart from that, there is also a chance for reducing the hotspots inside the combustion chamber which reduces the risk of backfire (Verhelst and Wallner, 2009).

6. Conclusions

This article has critically reviewed the hydrogen–gasoline dual fuel approach for SI engines. The dual fuel concept is an efficient potential approach for utilizing gaseous renewable fuels in SI engines. In addition, the dual fuel concept offers broad flexibility in governing the combustion process by combining the unique advantages of PFI and DI technologies and is an effective approach to achieving strict emission standards. Compared to conventional SI engines, dual fuel engines possess wide flexibility in mixture formation, enhanced cooling effect, knock mitigation, and emission reductions. Hydrogen has drawn the attention of many researchers for use as a dual fuel along with gasoline, more than any other renewable fuel. Dual fuel engines have the provision for introducing renewable fuels via either DI or PFI. However, hydrogen DI and gasoline PFI are optimal for enhancing engine performance.

In hydrogen DI, the abnormal combustion such as preignition, backfire and knock can be reduced compared to hydrogen PFI. But in terms of emission, higher amount of NO_x and increase in cyclic variation is observed. The combustion, performance, cyclic variation, and emission characteristics of the hydrogen–gasoline dual fuel engine have been reviewed from past works and show that hydrogen enrichment improves an SI engine's overall efficiency and performance. The wide flammability and rapid flame speed of hydrogen has reduced the combustion duration and increased the engine speed where the physical and chemical delays are reduced which enhanced the cold start properties. Hydrogen addition showed improvements in thermal efficiency and brake power which are most pronounced at low and partial loads. Even with a small amount of hydrogen enrichment an increase of 13% in engine torque was obtained. The lean conditions are further extended with hydrogen addition which showed a drastic reduction in CO and HC emissions. The incorporation of EGR showed better result in NO_x reduction. Increasing the EGR flowrate has resulted with a maximum NO_x reduction of 77.8% with 18% EGR flow rate. Further increment in EGR resulted in combustion instability as well as in HC and CO emissions.

The high auto-ignition temperature of hydrogen limits its use as a single fuel in the CI engines, which otherwise requires glow plug or spark plug for hydrogen combustion. So, introducing hydrogen to SI engine is the best approach to address the twin alarming global issues. Abnormal combustion like knock, preignition and backfire are more associated with hydrogen fuel. This limits the hydrogen fraction to increase beyond a certain point, which results in reduced engine performance at high engine load. This power deterioration at high load is addressed using dual fuel method along with use of conventional fossil fuels. Even though dual fuel method provides an extensible solution, approaches which can be used to further extend the hydrogen fraction over conventional fossil fuel is of prime importance, where detailed literature is still missing. The approaches for preventing the back flow of high temperature gas from the combustion chamber to intake manifold, reduction of in-cylinder hotspots like hot spark plug, residual high temperature carbon deposits and maintaining the incoming air–fuel temperature below auto-ignition temperature can be used to reduce the risk of abnormal combustion associated with the hydrogen fuel.

Declaration of competing interest

The authors declare that they have no known competing financial interests or personal relationships that could have appeared to influence the work reported in this paper.

Data availability

No data was used for the research described in the article.

Acknowledgments

FUNDING: This work was supported by the United Arab Emirates University, fund number 2N088 and fund number 31R165.

References

Abdalla, A.M., Hossain, S., Nisfindy, O.B., Azad, A.T., Dawood, M., Azad, A.K., 2018. Hydrogen production, storage, transportation and key challenges with applications: A review. Energy Convers. Manag. 165, 602–627.
Aghahasani, M., Gharehghani, A., Mahmoudzadeh Andwari, A., Mikulski, M., Pesyridis, A., Megaritis, T., et al., 2022. Numerical study on hydrogen–gasoline dual-fuel spark ignition engine. Processes 10 (11), 2249.
Akal, D., Öztuna, S., Büyükakın, M.K., 2020. A review of hydrogen usage in internal combustion engines (gasoline-lpg-diesel) from combustion performance aspect. Int. J. Hydrog. Energy. 45 (60), 35257–35268.
Akande, O., Lee, B., 2022. Plasma steam methane reforming (PSMR) using a microwave torch for commercial-scale distributed hydrogen production. Int. J. Hydrog. Energy. 47 (5), 2874–2884.
Al-Baghdadi, MA-RS., 2002. A study on the hydrogen–ethyl alcohol dual fuel spark ignition engine. Energy Convers. Manag. 43 (2), 199–204.
Alam, M., Goto, S., Sugiyama, K., Kajiwara, M., Mori, M., Konno, M., et al., 2001. Performance and emissions of a DI diesel engine operated with LPG and ignition improving additives. SAE Trans. 2446–2454.
Amirabedi, M., Jafarmadar, S., Khalilarya, S., 2019. Experimental investigation the effect of Mn2O3 nanoparticle on the performance and emission of SI gasoline fueled with mixture of ethanol and gasoline. Appl. Therm. Eng. 149, 512–519.
Antunes, J.M.G., Mikalsen, R., Roskilly, A.P., 2008. An investigation of hydrogen-fuelled HCCI engine performance and operation. Int. J. Hydrog. Energy. 33 (20), 5823–5828.
Ashok, B., Ashok, S.D., Kumar, C.R., 2015. LPG diesel dual fuel engine–a critical review. Alex. Eng. J. 54 (2), 105–126.
BAŞ, Oğuz, Akar, M.A., Serin, H., 2020. Reducing emissions of an SI engine by alternative spark plugs with hydrogen addition and variable compression ratio. Int. J. Automot. Eng. Technol. 9 (2), 94–104.
Bae, C., Kim, J., 2017. Alternative fuels for internal combustion engines. Proc. Combust. Inst. 36 (3), 3389–3413.
Baillie, D.C., 2010. Noise and vibration refinement of powertrain systems in vehicles. In: Vehicle Noise and Vibration Refinement. Elsevier, pp. 252–285.
Beretta, G.P., Rashidi, M., Keck, J.C., 1983. Turbulent flame propagation and combustion in spark ignition engines. Combust. Flame. 52, 217–245.
Bhola, D.R., 2011. CFD analysis of flow through venturi of carburetor.
Catapano, F., Di Iorio, S., Sementa, P., Vaglieco, B.M., 2016. Analysis of energy efficiency of methane and hydrogen-methane blends in a PFI/DI si research engine. Energy 117, 378–387.
Ceper, B.A., Akansu, S.O., Kahraman, N., 2009. Investigation of cylinder pressure for H2/CH4 mixtures at different loads. Int. J. Hydrog. Energy. 34 (11), 4855–4861.
Ceviz, M.A., Sen, A.K., Küleri, A.K., Öner, İV., 2012. Engine performance exhaust emissions, and cyclic variations in A lean-burn SI engine fueled by gasoline–hydrogen blends. Appl. Therm. Eng. 36, 314–324.
Chang, A.C.C., Chang, H.-F., Lin, F.-J., Lin, K.-H., Chen, C.-H., 2011. Biomass gasification for hydrogen production. Int. J. Hydrog. Energy. 36 (21), 14252–14260.
Chen, Z., Deng, J., Zhen, H., Wang, C., Wang, L., 2022. Experimental investigation of hydrous ethanol gasoline on engine noise, cyclic variations and combustion characteristics. Energies 15 (5), 1760.
Chen, L., Xu, F., Stone, R., Richardson, D., 2011. Spray imaging, mixture preparation and particulate matter emissions using a GDI engine fuelled with stoichiometric gasoline/ethanol blends. In: Conference on Internal Combustion Engines-Improving Performance. In: Fuel Economy Emissions, London, pp. 43–52.
Chi, J., Yu, H., 2018. Water electrolysis based on renewable energy for hydrogen production. Chin. J. Catal. 39 (3), 390–394.
Coronado, C.J.R., Carvalho, Jr., JA., Andrade, J.C., Cortez, E.V., Carvalho, F.S., Santos, J.C., et al., 2012. Flammability limits: A review with emphasis on ethanol for aeronautical applications and description of the experimental procedure. J. Hazard Mater. 241, 32–54.

da Costa, RBR., Hernandez, J.J., Teixeira, A.F., Netto, N.A.D., Valle, R.M., Roso, V.R., et al., 2019. Combustion, performance and emission analysis of a natural gas-hydrous ethanol dual-fuel spark ignition engine with internal exhaust gas recirculation. Energy Convers. Manag. 195, 1187–1198.

D'amato, G., Pawankar, R., Vitale, C., Lanza, M., Molino, A., Stanziola, A., et al., 2016. Climate change and air pollution: Effects on respiratory allergy. Allergy Asthma Immunol. Res. 8 (5), 391–395.

D'andrea, T., Henshaw, P.F., Ting, D.-K., 2004. The addition of hydrogen to a gasoline-fuelled SI engine. Int. J. Hydrog. Energy. 29 (14), 1541–1552.

Das, L.M., 1991. Exhaust emission characterization of hydrogen-operated engine system: Nature of pollutants and their control techniques. Int. J. Hydrog. Energy. 16 (11), 765–775.

Dhyani, V., Subramanian, K.A., 2018. Experimental investigation on effects of knocking on backfire and its control in a hydrogen fueled spark ignition engine. Int. J. Hydrog. Energy. 43 (14), 7169–7178.

Dhyani, V., Subramanian, K.A., 2019. Control of backfire and NOx emission reduction in a hydrogen fueled multi-cylinder spark ignition engine using cooled EGR and water injection strategies. Int. J. Hydrog. Energy. 44 (12), 6287–6298.

Dhyani, V., Subramanian, K.A., 2021. Development of online control system for elimination of backfire in a hydrogen fuelled spark ignition engine. Int. J. Hydrog. Energy. 46 (27), 14757–14763.

Dong, C., Zhou, Q., Zhao, Q., Zhang, Y., Xu, T., Hui, S., 2009. Experimental study on the Laminar flame speed of hydrogen/carbon monoxide/air mixtures. Fuel 88 (10), 1858–1863.

Du, Y., Yu, X., Liu, L., Li, R., Zuo, X., Sun, Y., 2017. Effect of addition of hydrogen and exhaust gas recirculation on characteristics of hydrogen gasoline engine. Int. J. Hydrog. Energy. 42 (12), 8288–8298.

Du, Y., Yu, X., Wang, J., Wu, H., Dong, W., Gu, J., 2016. Research on combustion and emission characteristics of a lean burn gasoline engine with hydrogen direct-injection. Int. J. Hydrog. Energy. 41 (4), 3240–3248.

Duan, J., Liu, F., Sun, B., 2014. Backfire control and power enhancement of a hydrogen internal combustion engine. Int. J. Hydrog. Energy. 39 (9), 4581–4589.

Eckermann, E., 2001. World History of the Automobile. SAE.

El-Kassaby, M.M., Eldrainy, Y.A., Khidr, M.E., Khidr, K.I., 2016. Effect of hydroxy (HHO) gas addition on gasoline engine performance and emissions. Alex. Eng. J. 55 (1), 243–251.

Elnajjar, E., Al-Omari, S.A.B., Selim, M.Y.E., Purayil, STP., 2021a. CI engine performance and emissions with waste cooking oil biodiesel boosted with hydrogen supplement under different load and engine parameters. Alex. Eng. J..

Elnajjar, E., Selim, M.Y.E., Hamdan, M.O., 2013. Experimental study of dual fuel engine performance using variable LPG composition and engine parameters. Energy Convers. Manag. 76, 32–42.

Elnajjar, E., Syam, M.M., Al-Omari, SAB., 2021b. Experimental investigations of bio-syngas production using microwave pyrolysis of UAE's palm date seed pits. Fuel 303, 121348.

Elsemary, I.M.M., Attia, A.A.A., Elnagar, K.H., Elaraqy, AAM., 2016. Experimental investigation on performance of single cylinder spark ignition engine fueled with hydrogen-gasoline mixture. Appl. Therm. Eng. 106, 850–854.

Elsemary, I.M.M., Attia, A.A.A., Elnagar, K.H., Elsaleh, M.S., 2017. Spark timing effect on performance of gasoline engine fueled with mixture of hydrogen–gasoline. Int. J. Hydrog. Energy. 42 (52), 30813–30820.

Elwardany, A.E., Abouarida, O.E., Abdel-Rahman, A.A., 2021. A combined effect of stoichiometric-oxygen-hydrogen gas and alumina nanoparticles on CI engine operating characteristics. Fuel 296, 120705.

Essuman, S.P.K., Nyamful, A., Agbodemegbe, V., Debrah, S.K., 2019. Experimental studies of the effect of electrolyte strength, voltage and time on the production of brown's (HHO) gas using oxyhydrogen generator. Open J. Energy Effic. 8 (02), 64.

Feng, D., Wei, H., Pan, M., Zhou, L., Hua, J., 2018. Combustion performance of dual-injection using n-butanol direct-injection and gasoline port fuel-injection in a SI engine. Energy 160, 573–581.

Feng, H., Zhang, H., Wei, J., Li, B., Wang, D., 2019. The influence of mixing ratio of low carbon mixed alcohols on knock combustion of spark ignition engines. Fuel 240, 339–348.

Galloni, E., 2009. Analyses about parameters that affect cyclic variation in a spark ignition engine. Appl. Therm. Eng. 29 (5–6), 1131–1137.

Ganesan, N., Sahni, I., Samuel, O.D., Enweremadu, C.C., Veza, I., Chandran, D., 2022. Optimization and sustainability of gasohol/hydrogen blends for operative spark ignition engine utilization and green environment. Case Stud. Therm. Eng. 39, 102381.

Gao, J., Wang, X., Song, P., Tian, G., Ma, C., 2022. Review of the backfire occurrences and control strategies for port hydrogen injection internal combustion engines. Fuel 307, 121553.

Geo, V.E., Nagarajan, G., Nagalingam, B., 2008. Studies on dual fuel operation of rubber seed oil and its bio-diesel with hydrogen as the inducted fuel. Int. J. Hydrog. Energy. 33 (21), 6357–6367.

Göktaş, M., Balki, M.K., Sayin, C., Canakci, M., 2021. An evaluation of the use of alcohol fuels in SI engines in terms of performance, emission and combustion characteristics: A review. Fuel 286, 119425.

Gölcü, M., Sekmen, Y., Erduranlı, P., Salman, M.S., 2005. Artificial neural-network based modeling of variable valve-timing in a spark-ignition engine. Appl. Energy. 81 (2), 187–197.

Gong, C., Li, Z., Huang, K., Liu, F., 2020. Research on the performance of a hydrogen/methanol dual-injection assisted spark-ignition engine using late-injection strategy for methanol. Fuel 260, 116403.

Gong, C., Liu, Z., Su, H., Chen, Y., Li, J., Liu, F., 2019. Effect of injection strategy on cold start firing, combustion and emissions of a LPG/methanol dual-fuel spark-ignition engine. Energy 178, 126–133.

Grahame, T.J., Schlesinger, R.B., 2010. Cardiovascular health and particulate vehicular emissions: A critical evaluation of the evidence. Air Qual. Atmos. Heal. 3 (1), 3–27.

Gurz, M., Baltacioglu, E., Hames, Y., Kaya, K., 2017. The meeting of hydrogen and automotive: A review. Int. J. Hydrog. Energy. 42 (36), 23334–23346.

Hagos, F.Y., Aziz, A.R.A., Sulaiman, S.A., 2014. Effect of air-fuel ratio on the combustion characteristics of syngas (H2: CO) in direct-injection spark-ignition engine. Energy Procedia. 61, 2567–2571.

Hamdan, M.O., Martin, P., Elnajjar, E., Selim, M.Y.E., Al-Omari, S., 2014. Diesel engine performance and emission under hydrogen supplement. In: ICREGA'14-Renewable Energy: Generation and Applications. Springer, pp. 329–337.

Hamdan, M.O., Selim, M.Y.E., Al-Omari, S.-A., Elnajjar, E., 2015. Hydrogen supplement co-combustion with diesel in compression ignition engine. Renew. Energy. 82, 54–60.

Hao, L., Xu, X., Guo, X., Ji, C., Wang, X., Tan, J., et al., 2016. Investigation of cold-start emission control strategy for a bi-fuel hydrogen/gasoline engine. Int. J. Hydrog. Energy. 41 (40), 18273–18281.

Hermesmann, M., Müller, T.E., 2022. Green, turquoise, blue, or grey? Environmentally friendly hydrogen production in transforming energy systems. Prog. Energy Combust. Sci. 90, 100996.

Heywood, J.B., 2018. Internal Combustion Engine Fundamentals. McGraw-Hill Education.

Holladay, J.D., Hu, J., King, D.L., Wang, Y., 2009. An overview of hydrogen production technologies. Catal. Today. 139 (4), 244–260.

Huang, Y., Surawski, N.C., Zhuang, Y., Zhou, J.L., Hong, G., 2021. Dual injection: An effective and efficient technology to use renewable fuels in spark ignition engines. Renew. Sustain. Energy Rev. 143, 110921.

Ikeda, Y., Kawahara, N., 2022. Measurement of cyclic variation of the air-to-fuel ratio of exhaust gas in an SI engine by laser-induced breakdown spectroscopy. Energies 15 (9), 3053.

Jamrozik, A., Tutak, W., 2011. A study of performance and emissions of SI engine with a two-stage combustion system. Chem Process Eng. 453–471.

Ji, C., Cong, X., Wang, S., Shi, L., Su, T., Wang, D., 2018. Performance of a hydrogen-blended gasoline direct injection engine under various second gasoline direct injection timings. Energy Convers. Manag. 171, 1704–1711.

Ji, C., Liu, X., Gao, B., Wang, S., Yang, J., 2013. Numerical investigation on the combustion process in a spark-ignited engine fueled with hydrogen–gasoline blends. Int. J. Hydrog. Energy. 38 (25), 11149–11155.

Ji, C., Shi, C., Wang, S., Yang, J., Su, T., Wang, D., 2019. Effect of dual-spark plug arrangements on ignition and combustion processes of a gasoline rotary engine with hydrogen direct-injection enrichment. Energy Convers. Manag. 181, 372–381.

Ji, C., Wang, S., 2011. Effect of hydrogen addition on lean burn performance of a spark-ignited gasoline engine at 800 rpm and low loads. Fuel 90 (3), 1301–1304.

Ji, C., Wang, S., Zhang, B., 2010. Effect of spark timing on the performance of a hybrid hydrogen–gasoline engine at lean conditions. Int. J. Hydrog. Energy. 35 (5), 2203–2212.

Ji, C., Wang, S., Zhang, B., 2012. Performance of a hybrid hydrogen–gasoline engine under various operating conditions. Appl. Energy. 97, 584–589.

Jilakara, S., Vaithianathan, J.V., Natarajan, S., Ramakrishnan, V.R., Subash, G.P., Abraham, M., et al., 2015. An experimental study of turbocharged hydrogen fuelled internal combustion engine. SAE Int. J. Engines. 8 (1), 314–325.

Jolly, W.L., 2021. Hydrogen. In: Encycl Br [Internet]. Available from: https://www.britannica.com/science/hydrogen.

Kahraman, N., Ceper, B., Akansu, S.O., Aydin, K., 2009. Investigation of combustion characteristics and emissions in a spark-ignition engine fuelled with natural gas–hydrogen blends. Int. J. Hydrog. Energy. 34 (2), 1026–1034.

Kakoulaki, G., Kougias, I., Taylor, N., Dolci, F., Moya, J., Jäger-Waldau, A., 2021. Green hydrogen in europe–a regional assessment: Substituting existing production with electrolysis powered by renewables. Energy Convers. Manag. 228, 113649.

Kaleli, A., Ceviz, M.A., Erenturk, K., 2015. Controlling spark timing for consecutive cycles to reduce the cyclic variations of SI engines. Appl. Therm. Eng. 87, 624–632.

Kalghatgi, G., 2019. Development of fuel/engine systems—the way forward to sustainable transport. Engineering 5 (3), 510–518.

Kalwar, A., Agarwal, A.K., 2020. Overview, advancements and challenges in gasoline direct injection engine technology. In: Advanced Combustion Techniques and Engine Technologies for the Automotive Sector. Springer, pp. 111–147.
Kamil, M., Rahman, M.M., 2015. Performance prediction of spark-ignition engine running on gasoline-hydrogen and methane-hydrogen blends. Appl. Energy 158, 556–567.
Kang, R., Zhou, L., Hua, J., Feng, D., Wei, H., Chen, R., 2019. Experimental investigation on combustion characteristics in dual-fuel dual-injection engine. Energy Convers. Manag. 181, 15–25.
Kasseris, E., Heywood, J., 2012. Charge cooling effects on knock limits in SI DI engines using gasoline/ethanol blends: Part 2-effective octane numbers. SAE Int. J. Fuels Lubr. 5 (2), 844–854.
Kim, N., Cho, S., Choi, H., Song, H.H., Min, K., 2014. The Efficiency and Emission Characteristics of Dual Fuel Combustion using Gasoline Direct Injection and Ethanol Port Injection in an SI Engine. SAE Technical Paper.
Kim, J., Chun, K.M., Song, S., Baek, H.-K., Lee, S.W., 2017. The effects of hydrogen on the combustion, performance and emissions of a turbo gasoline direct-injection engine with exhaust gas recirculation. Int. J. Hydrog. Energy. 42 (39), 25074–25087.
Kim, J., Chun, K.M., Song, S., Baek, H.-K., Lee, S.W., 2018. Hydrogen effects on the combustion stability, performance and emissions of a turbo gasoline direct injection engine in various air/fuel ratios. Appl. Energy. 228, 1353–1361.
Kim, J., Chun, K.M., Song, S., Baek, H.-K., Lee, S.W., 2020. Improving the thermal efficiency of a T-GDI engine using hydrogen from combined steam and partial oxidation exhaust gas reforming of gasoline under low-load stoichiometric conditions. Fuel 273, 117754.
Kim, K.-H., Kabir, E., Kabir, S., 2015. A review on the human health impact of airborne particulate matter. Environ. Int. 74, 136–143.
Kim, A., Lee, H., Brigljević, B., Yoo, Y., Kim, S., Lim, H., 2021. Thorough economic and carbon footprint analysis of overall hydrogen supply for different hydrogen carriers from overseas production to Inland distribution. J. Clean. Prod. 316, 128326.
Kumar, V., Gupta, D., Kumar, N., 2015. Hydrogen use in internal combustion engine: A review. Int. J. Adv. Cult. Technol. 3 (2), 87–99.
Kumar, R.S., Purayil, STP., 2019. Optimization of ethyl ester production from arachis hypogaea oil. Energy Rep. 5, 658–665.
Lapuerta, M., Hernández, J.P., Agudelo, J.R., 2014. An equation for the estimation of alcohol-air diffusion coefficients for modelling evaporation losses in fuel systems. Appl. Therm. Eng. 73 (1), 539–548.
Lee, Z., Kim, T., Park, S., Park, S., 2020. Review on spray, combustion, and emission characteristics of recent developed direct-injection spark ignition (DISI) engine system with multi-hole type injector. Fuel 259, 116209.
Lee, J., Lee, S., Lee, S., 2018. Experimental investigation on the performance and emissions characteristics of ethanol/diesel dual-fuel combustion. Fuel 220, 72–79.
LeValley, T.L., Richard, A.R., Fan, M., 2014. The progress in water gas shift and steam reforming hydrogen production technologies–a review. Int. J. Hydrog. Energy. 39 (30), 16983–17000.
Li, G., Yu, X., Jin, Z., Shang, Z., Li, D., Li, Y., et al., 2020. Study on effects of split injection proportion on hydrogen mixture distribution, combustion and emissions of a gasoline/hydrogen SI engine with split hydrogen direct injection under lean burn condition. Fuel 270, 117488.
Li, G., Zhang, C., Zhou, J., 2017. Study on the knock tendency and cyclical variations of a HCCI engine fueled with n-butanol/n-heptane blends. Energy Convers. Manag. 133, 548–557.
Liang, J., 2019. Effects of air-fuel ratio and hydrogen fraction on combustion characteristics of hydrogen direct-injection gasoline engine. In: IOP Conference Series: Earth and Environmental Science. IOP Publishing, p. 42012.
Liu, Z., Yu, X., Sun, P., Xu, S., 2021. Experimental investigation of the performance and emissions of a dual-injection SI engine with natural gas direct injection plus gasoline port injection under lean-burn conditions. Fuel 300, 120952.
Log, T., Moi, A.L., 2018. Ethanol and methanol burn risks in the home environment. Int. J. Environ. Res. Public Health. 15 (11), 2379.
Lu, S., Zhao, B., Chen, M., Wang, L., Fu, X.-Z., Luo, J.-L., 2020. Electrolysis of waste water containing aniline to produce polyaniline and hydrogen with low energy consumption. Int. J. Hydrog. Energy. 45 (43), 22419–22426.
Ma, F., Wang, Y., 2008. Study on the extension of lean operation limit through hydrogen enrichment in a natural gas spark-ignition engine. Int. J. Hydrog. Energy. 33 (4), 1416–1424.
Manigandan, S., Gunasekar, P., Poorchilamban, S., Nithya, S., Devipriya, J., Vasanthkumar, G., 2019. Effect of addition of hydrogen and TiO2 in gasoline engine in various exhaust gas recirculation ratio. Int. J. Hydrog. Energy. 44 (21), 11205–11218.
Martinez, S., Merola, S., Irimescu, A., 2019. Flame front and burned gas characteristics for different split injection ratios and phasing in an optical GDI engine. Appl. Sci. 9 (3), 449.
Masum, B.M., Masjuki, H.H., Kalam, M.A., Palash, Sm, Habibullah, M., 2015. Effect of alcohol–gasoline blends optimization on fuel properties, performance and emissions of a SI engine. J. Clean. Prod. 86, 230–237.
Melaika, M., Herbillon, G., Dahlander, P., 2021. Spark ignition engine performance, standard emissions and particulates using GDI, PFI-CNG and DI-CNG systems. Fuel 293, 120454.
Midilli, A., Kucuk, H., Topal, M.E., Akbulut, U., Dincer, I., 2021. A comprehensive review on hydrogen production from coal gasification: Challenges and opportunities. Int. J. Hydrog. Energy. 46 (50), 25385–25412.
Milewski, J., Kupecki, J., Szczęśniak, A., Uzunow, N., 2021. Hydrogen production in solid oxide electrolyzers coupled with nuclear reactors. Int. J. Hydrog. Energy. 46 (72), 35765–35776.
Muradov, N.Z., 1993. How to produce hydrogen from fossil fuels without CO2 emission. Int. J. Hydrog. Energy. 18 (3), 211–215.
Navale, S.J., Kulkarni, R.R., Thipse, S.S., 2017. An experimental study on performance, emission and combustion parameters of hydrogen fueled spark ignition engine with the timed manifold injection system. Int. J. Hydrog. Energy. 42 (12), 8299–8309.
Nguyen, D.-K., 2013. Improving performance and reducing pollution emissions of a carburetor gasoline engine by adding HHO gas into th.
Nguyen, D., Choi, Y., Park, C., Kim, Y., Lee, J., 2021. Effect of supercharger system on power enhancement of hydrogen-fueled spark-ignition engine under low-load condition. Int. J. Hydrog. Energy. 46 (9), 6928–6936.
Niu, R., Yu, X., Du, Y., Xie, H., Wu, H., Sun, Y., 2016. Effect of hydrogen proportion on lean burn performance of a dual fuel SI engine using hydrogen direct-injection. Fuel 186, 792–799.
Nwovu, S.O., Cairns, A., Vafamehr, H., 2018. Effects of direct injection DI on knocking combustion in spark ignition SI engine operated on 75-RON and ethanol fuels. In: SPE Nigeria Annual International Conference and Exhibition. OnePetro.
Pai, S., Tasneem, H.R.A., Rao, A., Shivaraju, N., Sreeprakash, B., 2013. Study of impact of ethanol blends on SI engine performance and emission. In: National Conference on Challenges in Research & Technology in the Coming Decades. CRT 2013, IET, pp. 1–7.
Pandey, J.K., Kumar, G.N., 2022. Effect of variable compression ratio and equivalence ratio on performance, combustion and emission of hydrogen port injection SI engine. Energy 239, 122468.
Pein, M., Neumann, N.C., Venstrom, L.J., Vieten, J., Roeb, M., Sattler, C., 2021. Two-step thermochemical electrolysis: An approach for green hydrogen production. Int. J. Hydrog. Energy..
Qian, L., Wan, J., Qian, Y., Sun, Y., Zhuang, Y., 2022. Experimental investigation of water injection and spark timing effects on combustion and emissions of a hybrid hydrogen-gasoline engine. Fuel 322, 124051.
Rana, K.K., Natarajan, S., Jilakara, S., 2015. Potential of hydrogen fuelled IC engine to achieve the future performance and emission norms.
Reitz, R.D., Ogawa, H., Payri, R., Fansler, T., Kokjohn, S., Moriyoshi, Y., et al., 2020. IJER Editorial: The Future of the Internal Combustion Engine. SAGE Publications Sage, UK,London, England.
Sahu, S.C., Hayes, A.W., 2017. Toxicity of nanomaterials found in human environment: A literature review. Toxicol. Res. Appl. 1, 2397847317726352.
Sáinz, D., Diéguez, P.M., Sopena, C., Urroz, J.C., Gandía, L.M., 2012. Conversion of a commercial gasoline vehicle to run bi-fuel (hydrogen-gasoline). Int. J. Hydrog. Energy. 37 (2), 1781–1789.
Salazar, V., Kaiser, S., 2011. Influence of the flow field on flame propagation in a hydrogen-fueled internal combustion engine. SAE Int. J. Engines. 4 (2), 2376–2394.
Salek, F., Babaie, M., Hosseini, S.V., Bég, O.A., 2021. Multi-objective optimization of the engine performance and emissions for a hydrogen/gasoline dual-fuel engine equipped with the port water injection system. Int. J. Hydrog. Energy. 46 (17), 10535–10547.
Sanni, S.E., Alaba, P.A., Okoro, E., Emetere, M., Oni, B., Agboola, O., et al., 2021. Strategic examination of the classical catalysis of formic acid decomposition for intermittent hydrogen production, storage and supply: A review. Sustain. Energy Technol. Assess. 45, 101078.
Santos, ND.S.A., Alvarez, C.E.C., Roso, V.R., Baeta, J.G.C., Valle, R.M., 2019. Combustion analysis of a SI engine with stratified and homogeneous pre-chamber ignition system using ethanol and hydrogen. Appl. Therm. Eng. 160, 113985.
Santos, J.L., Megías-Sayago, C., Ivanova, S., MÁ, Centeno., Odriozola, J.A., 2021. Functionalized biochars as supports for Pd/C catalysts for efficient hydrogen production from formic acid. Appl. Catal. B Environ. 282, 119615.
Sarma, S.J., Brar, S.K., Sydney, E.B., Le Bihan, Y., Buelna, G., Soccol, C.R., 2012. Microbial hydrogen production by bioconversion of crude glycerol: A review. Int. J. Hydrog. Energy. 37 (8), 6473–6490.
Sharifi, S., Behzadi, S., Laurent, S., Forrest, M.L., Stroeve, P., Mahmoudi, M., 2012. Toxicity of nanomaterials. Chem. Soc. Rev. 41 (6), 2323–2343.
Sharma, R., Almáši, M., Nehra, S.P., Rao, V.S., Panchal, P., Paul, D.R., et al., 2022. Photocatalytic hydrogen production using graphitic carbon nitride (GCN): A precise review. Renew. Sustain. Energy Rev. 168, 112776.
Sharma, S., Ghoshal, S.K., 2015. Hydrogen the future transportation fuel: From production to applications. Renew. Sustain. Energy Rev. 43, 1151–115s8.
Sharma, M., Kaushal, R., 2021. Performance and exhaust emission analysis of a variable compression ratio (VCR) dual fuel CI engine fuelled with producer gas generated from pistachio shells. Fuel 283, 118924.

Sheu, W.-J., Chu, C.-S., Chen, Y.-C., 2021. The operation types and operation window for high-purity hydrogen production for the sorption enhanced steam methane reforming in a fixed-bed reactor. Int. J. Hydrog. Energy..
Shi, W., Yu, X., Zhang, H., Li, H., 2017. Effect of spark timing on combustion and emissions of a hydrogen direct injection stratified gasoline engine. Int. J. Hydrog. Energy. 42 (8), 5619–5626.
Shivaprasad, K.V., Raviteja, S., Chitragar, P., Kumar, G.N., 2014. Experimental investigation of the effect of hydrogen addition on combustion performance and emissions characteristics of a spark ignition high speed gasoline engine. Procedia Technol. 14, 141–148.
Shuai, S., Ma, X., Li, Y., Qi, Y., Xu, H., 2018. Recent progress in automotive gasoline direct injection engine technology. Automot. Innov. 1 (2), 95–113.
Siddiqui, O., Dincer, I., 2021. Design and assessment of a new solar-based biomass gasification system for hydrogen, cooling, power and fresh water production utilizing rice husk biomass. Energy Convers. Manag. 236, 114001.
Silva, P.P., Ferreira, R.A.R., Noronha, F.B., Hori, C.E., 2017. Hydrogen production from steam and oxidative steam reforming of liquefied petroleum gas over cerium and strontium doped LaNiO3 catalysts. Catal Today. 289, 211–221.
Singh, E., Morganti, K., Dibble, R., 2019. Dual-fuel operation of gasoline and natural gas in a turbocharged engine. Fuel 237, 694–706.
Sinigaglia, T., Lewiski, F., Martins, M.E.S., Siluk, JCM., 2017. Production, storage, fuel stations of hydrogen and its utilization in automotive applications-a review. Int. J. Hydrog. Energy. 42 (39), 24597–24611.
Steinbrecher, C., Hamedovic, H., Rupp, A., Wortmann, T., 2016. Improved fuel metering for port fuel injection by controlled valve operation. SAE Int. J. Engines. 9 (4), 2460–2468.
Stępień, Z., 2021. A comprehensive overview of hydrogen-fueled internal combustion engines: Achievements and future challenges. Energies 14 (20), 6504.
Su, T., Ji, C., Wang, S., Cong, X., Shi, L., 2018. Improving the combustion performance of a gasoline rotary engine by hydrogen enrichment at various conditions. Int. J. Hydrog. Energy. 43 (3), 1902–1908.
Su, T., Ji, C., Wang, S., Shi, L., Yang, J., Cong, X., 2017a. Effect of spark timing on performance of a hydrogen-gasoline rotary engine. Energy Convers. Manag. 148, 120–127.
Su, T., Ji, C., Wang, S., Shi, L., Yang, J., Cong, X., 2017b. Idle performance of a hydrogen/gasoline rotary engine at lean condition. Int. J. Hydrog. Energy. 42 (17), 12696–12705.
Su, T., Ji, C., Wang, S., Shi, L., Yang, J., Cong, X., 2017c. Investigation on performance of a hydrogen-gasoline rotary engine at part load and lean conditions. Appl. Energy. 205, 683–691.
Subramaniam, M., Satish, S., Solomon, J.M., Sathyamurthy, R., 2020. Numerical and experimental investigation on capture of CO2 and other pollutants from an SI engine using the physical adsorption technique. Heat Transf. 49 (5), 2943–2960.
Subramanian, B., Thangavel, V., 2020. Experimental investigations on performance, emission and combustion characteristics of diesel-hydrogen and diesel-HHO gas in a dual fuel CI engine. Int. J. Hydrog. Energy. 45 (46), 25479–25492.
Sun, P., Liu, Z., Yu, X., Yao, C., Guo, Z., Yang, S., 2019. Experimental study on heat and exergy balance of a dual-fuel combined injection engine with hydrogen and gasoline. Int. J. Hydrog. Energy. 44 (39), 22301–22315.
Sun, Y., Yu, X., Jiang, L., 2016. Effects of direct hydrogen injection on particle number emissions from a lean burn gasoline engine. Int. J. Hydrog. Energy. 41 (41), 18631–18640.
Szwaja, S., Bhandary, K.R., Naber, J.D., 2007. Comparisons of hydrogen and gasoline combustion knock in a spark ignition engine. Int. J. Hydrog. Energy. 32 (18), 5076–5087.
Taghavifar, H., Kaleji, B.K., Kheyrollahi, J., 2020. Application of composite TNA nanoparticle with bio-ethanol blend on gasoline fueled SI engine at different lambda ratios. Fuel 277, 118218.
Tesfa, B., Mishra, R., Zhang, C., Gu, F., Ball, A.D., 2013. Combustion and performance characteristics of CI (compression ignition) engine running with biodiesel. Energy 51, 101–115.
Thakur, A.K., Kaviti, A.K., Mehra, R., Mer, KKS., 2017. Progress in performance analysis of ethanol-gasoline blends on SI engine. Renew. Sustain. Energy Rev. 69, 324–340.
Uddin, M.N., Daud, WM.A.W., Abbas, H.F., 2014. Effects of pyrolysis parameters on hydrogen formations from biomass: A review. Rsc Adv. 4 (21), 10467–10490.
Vardar-Schara, G., Maeda, T., Wood, T.K., 2008. Metabolically engineered bacteria for producing hydrogen via fermentation. Microb. Biotechnol. 1 (2), 107–125.
Verhelst, S., Wallner, T., 2009. Hydrogen-fueled internal combustion engines. Prog. Energy Combust. Sci. 35 (6), 490–527.
Vinoth Kanna, I., Paturu, P., 2020. A study of hydrogen as an alternative fuel. Int. J. Ambient Energy 41 (12), 1433–1436.
Wang, S., Ji, C., 2012. Cyclic variation in a hydrogen-enriched spark-ignition gasoline engine under various operating conditions. Int. J. Hydrog. Energy. 37 (1), 1112–1119.
Wang, S., Ji, C., Zhang, B., 2010. Effects of hydrogen addition and cylinder cutoff on combustion and emissions performance of a spark-ignited gasoline engine under a low operating condition. Energy 35 (12), 4754–4760.
Wang, S., Ji, C., Zhang, B., 2011. Starting a spark-ignited engine with the gasoline–hydrogen mixture. Int. J. Hydrog. Energy. 36 (7), 4461–4468.
Wang, X., Meng, Q., Gao, L., Jin, Z., Ge, J., Liu, C., et al., 2018. Recent progress in hydrogen production from formic acid decomposition. Int. J. Hydrog. Energy. 43 (14), 7055–7071.
Wang, M., Wang, G., Sun, Z., Zhang, Y., Xu, D., 2019. Review of renewable energy-based hydrogen production processes for sustainable energy innovation. Glob. Energy Interconnect. 2 (5), 436–443.
White, C.M., Steeper, R.R., Lutz, A.E., 2006. The hydrogen-fueled internal combustion engine: A technical review. Int. J. Hydrog. Energy. 31 (10), 1292–1305.
Winterbone, Desmond E., Turan, Ali, 2015. Reciprocating internal combustion engines. Adv. Thermodyn. Eng. 345–379.
Yan, F., Xu, L., Wang, Y., 2018. Application of hydrogen enriched natural gas in spark ignition IC engines: From fundamental fuel properties to engine performances and emissions. Renew. Sustain. Energy Rev. 82, 1457–1488.
Yang, Z., Bandivadekar, A., 2017. Light-Duty Vehicle Greenhouse Gas and Fuel Economy Standards. ICCT Rep., p. 16.
Yang, Z., Du, Y., Geng, Q., He, G., 2022. Energy loss and comprehensive performance analysis of a novel high-efficiency hybrid cycle hydrogen-gasoline rotary engine under off-design conditions. Energy Convers. Manag. 267, 115942.
Yang, J., Ji, C., 2018. A comparative study on performance of the rotary engine fueled hydrogen/gasoline and hydrogen/n-butanol. Int. J. Hydrog. Energy. 43 (50), 22669–22675.
Yang, L., Zare, A., Bodisco, T.A., Nabi, N., Liu, Z., Brown, R.J., 2021. Analysis of cycle-to-cycle variations in a common-rail compression ignition engine fuelled with diesel and biodiesel fuels. Fuel 290, 120010.
Yilmaz, IT, 2021. The effect of hydrogen on the thermal efficiency and combustion process of the low compression ratio CI engine. Appl. Therm. Eng. 197, 117381.
Yilmaz, A.C., Uludamar, E., Aydin, K., 2010. Effect of hydroxy (HHO) gas addition on performance and exhaust emissions in compression ignition engines. Int. J. Hydrog. Energy. 35 (20), 11366–11372.
Yip, H.L., Srna, A., Yuen, A.C.Y., Kook, S., Taylor, R.A., Yeoh, G.H., et al., 2019. A review of hydrogen direct injection for internal combustion engines: Towards carbon-free combustion. Appl. Sci. 9 (22), 4842.
Yu, X., Du, Y., Sun, P., Liu, L., Wu, H., Zuo, X., 2017. Effects of hydrogen direct injection strategy on characteristics of lean-burn hydrogen–gasoline engines. Fuel 208, 602–611.
Yu, X., Guo, Z., He, L., Dong, W., Sun, P., Du, Y., et al., 2019a. Experimental study on lean-burn characteristics of an SI engine with hydrogen/gasoline combined injection and EGR. Int. J. Hydrog. Energy. 44 (26), 13988–13998.
Yu, X., Li, G., Du, Y., Guo, Z., Shang, Z., He, F., et al., 2019b. A comparative study on effects of homogeneous or stratified hydrogen on combustion and emissions of a gasoline/hydrogen SI engine. Int. J. Hydrog. Energy. 44 (47), 25974–25984.
Yu, X., Li, D., Yang, S., Sun, P., Guo, Z., Yang, H., et al., 2020. Effects of hydrogen direct injection on combustion and emission characteristics of a hydrogen/acetone-butanol-ethanol dual-fuel spark ignition engine under lean-burn conditions. Int. J. Hydrog. Energy. 45 (58), 34193–34203.
Yu, J., Takahashi, P., 2007. Biophotolysis-based hydrogen production by cyanobacteria and green microalgae. Commun. Curr. Res. Educ. Top. Trends Appl. Microbiol. 1, 79–89.
Yu, X., Wu, H., Du, Y., Tang, Y., Liu, L., Niu, R., 2016. Research on cycle-by-cycle variations of an SI engine with hydrogen direct injection under lean burn conditions. Appl. Therm. Eng. 109, 569–581.
Zaharin, M.S.M., Abdullah, N.R., Masjuki, H.H., Ali, O.M., Najafi, G., Yusaf, T., 2018. Evaluation on physicochemical properties of iso-butanol additives in ethanol-gasoline blend on performance and emission characteristics of a spark-ignition engine. Appl. Therm. Eng. 144, 960–971.
Zervas, E., Montagne, X., Lahaye, J., 2004. Impact of fuel composition on the emission of regulated pollutants and specific hydrocarbons from a SI engine. Tech. Chron. Sci. J. TCG. 1–2.
Zhang, Z., Feng, H., Zuo, Z., 2020. Numerical investigation of a free-piston hydrogen-gasoline engine linear generator. Energies 13 (18), 4685.
Zhang, M., Hong, W., Xie, F., Su, Y., Liu, H., Zhou, S., 2018. Combustion, performance and particulate matter emissions analysis of operating parameters on a GDI engine by traditional experimental investigation and Taguchi method. Energy Convers. Manag. 164, 344–352.
Zhen, X., Wang, Y., 2015. An overview of methanol as an internal combustion engine fuel. Renew. Sustain. Energy Rev. 52, 477–493.